Net ecosystem production of coral communities persisting under marginal environmental conditions

Timothy B. King[1], Yu-De Pei[1], Joshua Bennett-Williams[1], Alex S. J. Wyatt[1]

[1]Department of Ocean Science, The Hong Kong University of Science and Technology, Clear Water Bay, Kowloon, Hong Kong

Correspondence to: Alex S.J. Wyatt (wyatt@ust.hk)

Abstract. Coral communities in Hong Kong persist under a range of local stressors, including strong subtropical seasonality, chronic low light, and high turbidity, resulting in patchy, compositionally constrained communities relative to typical tropical reef systems. These challenging environmental conditions provide an opportunity to better understand how coral ecosystems may respond to changing ocean conditions in the future. Here, we used in-situ sensors to quantify high-resolution, community-scale net ecosystem production (NEP, organic carbon cycling) at three sites across a marine environmental gradient around Hong Kong. These communities were net respiring (negative NEP) across the gradient in both the wet (NEP_{mean}= -0.49 ± 4.83 mmol O_2 m^{-2} hr^{-1}) and dry seasons (NEP_{mean}= -0.21 ± 0.85 mmol O_2 m^{-2} hr^{-1}), with a significant increase in metabolic variability observed during the wet season (mean daily NEP range = 9.99 ± 13.34 mmol O_2 m^{-2} hr^{-1}) versus the dry season (2.38 ± 1.93 mmol O_2 m^{-2} hr^{-1}), associated with stronger variation in light and hydrographic conditions. This study adds to the small number of studies to date assessing in-situ metabolic variability of coral communities persisting under marginal environmental conditions. Understanding natural community-scale variability in organic carbon cycling is crucial for predicting how coral communities may cope with changing ocean conditions, thereby providing vital insights into the future of globally threatened coral ecosystems.

1 Introduction

Coral ecosystems offer crucial ecosystem services, such as supporting biodiversity hotspots, providing storm protection for coastal communities and tourism-related income (Moberg and Folke, 1999). However, the future viability of these ecosystems is threatened by a combination of global (Doney et al., 2009; Hughes et al., 2017) and local stressors (Tuttle and Donahue, 2022). We can better understand how coral communities might persist in the future by studying communities that are already surviving in challenging environments. While corals generally thrive in shallow, clear waters, coral ecosystems can persist under marginal environmental conditions and anthropogenic stressors (Schoepf et al., 2023), albeit typically with lower coral species diversity, slower growth rates, and without appreciable carbonate accretion (Heery et al., 2018). A key component of furthering understanding of how these corals are persisting in their environment is to understand how coral metabolic rates vary under local environmental stressors.

Corals in turbid, low-light environments, while having a compressed depth range (Morgan et al., 2020) and likely being more susceptible to sea-level rise due to higher light attenuation (Zweifler et al., 2021; Law and Huang, 2023), may be more resilient to future climate change due to shielding from heat and light stress (Morgan et al., 2017; Sully and Van Woesik, 2020; Rosedy et al., 2023) and may provide equal or even greater habitat capacity for associated organisms compared to clearer, higher coral cover reefs (Goatley and Bellwood 2011; Valino et al., 2026). These environments thus potentially serve as important climate refugia (Cacciapaglia and van Woesik, 2015). Hong Kong coral communities, which are subject to chronic low-light conditions and a compressed depth range (1-6 m, Goodkin et al., 2011), may serve as a proxy for understanding how coral communities may change function under more restricted geographic ranges and turbid conditions in the future (Zweifler et al., 2021).

In addition to low light, coral communities around Hong Kong persist under challenging environmental conditions resulting from the subtropical climatology and local anthropogenic forcing (Goodkin et al., 2011; Duprey et al., 2017). Hong Kong's subtropical, monsoonal climate varies markedly throughout the year. The wet season, which lasts from April to October, is marked by higher water temperatures (daily maximum of 32.4 °C, McIlroy et al., 2019), higher nutrient and sediment loads into coastal waters, more rainfall, and decreased salinity due to increased freshwater flux. The dry season, which lasts from November to March, is distinguished by low water temperatures (daily minimum of 14.7 °C, McIlroy et al., 2019), little rain, and higher salinities (Morton, 1989). Other local stressors, such as sea urchin-derived bioerosion (Dumont et al., 2013; Xie et al., 2020; Yeung et al., 2021), recreational activities (Chung et al., 2013), and elevated eutrophication rates (Duprey et al., 2016), fluctuate spatiotemporally around Hong Kong and can have short- and long-term impacts on the health of coral communities. An east-west environmental-urbanization gradient linked to human populations and discharge from the Pearl River disproportionally affects Hong Kong's western waters (Duprey et al., 2016; Cybulski et al., 2020). Therefore, most of Hong Kong's corals are now found farther away from the Pearl River Estuary, in the eastern, more oceanic waters of the territory (Duprey et al., 2020). High turbidity from elevated nutrients and sedimentation results in low-light conditions across Hong Kong. Despite these challenging environmental conditions, high coral cover areas can still be found in the eastern waters of Hong Kong. Therefore, coral communities in Hong Kong may be classified as 'marginal' for a variety of reasons, following the framework of Schoepf et al., (2023), depending on where they are located along the east-west environmental gradient. While the degree of structural marginality (coral cover, richness, community composition) can be more easily assessed with traditional benthic surveys, the functional marginality of a coral community can only be obtained through the quantification of a core process in coral community functioning (Brandl et al., 2019; Schoepf et al., 2023). In this study, we focus on net ecosystem production (NEP) as one measure of community-scale organic carbon cycling, allowing us to assess how this component of functional performance varies across the environmental gradient of Hong Kong.

A benthic community's NEP is proportional to the gradient in dissolved oxygen (DO) of the overlying seawater column (McGillis et al., 2011) and reflects the cycling of organic carbon and the balance between photosynthesis and respiration (Andersson and Gledhill, 2013). The magnitude of NEP generated by a benthic community can change over space

and time depending on the local biogeochemical environment, including benthic community composition (Page et al., 2019), and the physical environment, including increased residence time and wave action (Falter et al., 2012; Long et al., 2013). Photosynthesis increases dissolved oxygen through oxygen production, whereas respiration decreases dissolved oxygen through oxygen consumption; NEP reflects the net balance between these opposing processes (Turk et al., 2015; Lowe et al., 2019). Additionally, NEP will naturally fluctuate over diel to seasonal timescales and can be linked to the diversity of benthic communities (Takeshita et al., 2018), with more diverse and rich ecosystems tending to display greater metabolic variability (Page et al., 2017) and higher rates of net productivity (+NEP) (Odum and Odum, 1955; Long et al., 2013; Cyronak et al., 2018). In contrast, lower rates of NEP have been associated with more degraded reef environments (Kayanne et al., 2005; Takeshita et al., 2016; McMahon et al., 2019; Webb et al., 2021). Therefore, NEP can provide insight into one critical component of ecosystem function, namely community-scale organic carbon cycling (Allgeier, 2024). This community-scale variability has not been assessed in-situ in a highly urbanized coral environment like Hong Kong, which is subject to chronic local stressors.

Globally, community-scale organic metabolism over coral habitats remains under-examined (Platz et al., 2022). In Hong Kong, measurements of coral productivity have only been made at the level of individual corals (Dellisanti et al., 2020) or in mesocosm settings (McIlroy et al., 2019), with no assessments of in-situ NEP at a community scale. Community-scale NEP can change rapidly across small spatial scales, and the results of individual coral-scale metabolic rates may not be adequate for extrapolation to the community as a whole (Page et al., 2017). Understanding natural community-level variability is thus crucial for assessing how coral communities may change under future ocean conditions. Therefore, rather than extrapolating estimates from a single species, investigations should include the metabolic signal of the whole community (Edmunds et al., 2016) to better forecast how community organic carbon cycling may change in the future (Kekuewa et al., 2021). Accordingly, the main objectives of the study were to (1) characterize the natural spatiotemporal variability in coral community organic metabolism through in-situ NEP measurements along the environmental-urbanization gradient in Hong Kong, and (2) identify environmental factors that are the primary drivers of changes in NEP. Such information on the natural variability and environmental drivers of coral community-scale organic carbon cycling is essential to understand how corals will persist under shifting local and global ocean conditions, including increasing prevalence of marginal environmental conditions.

2 Materials and methods

2.1 Study sites

Three study sites were selected to represent a spectrum of environmental conditions around Hong Kong that still support corals, from east to west: Tung Ping Chau (22.5451°N, 114.4326°E), Sharp Island (22.3639°N, 114.2903°E), and Sham Wan (22.1861°N, 114.1359°E) (Fig. 1).

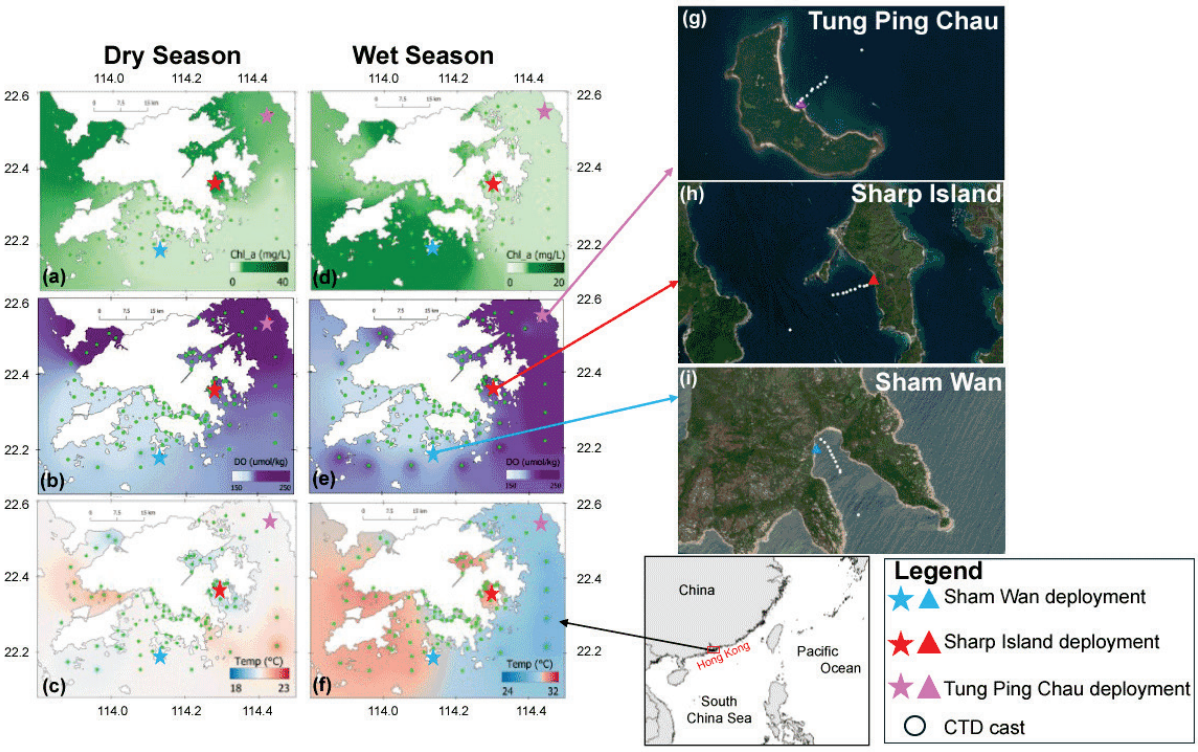

Figure 1. Marine spatial east-west environmental gradients and deployment locations around Hong Kong. Gradients during the dry (a, b, c; December 2021-January 2022) and wet (d, e, f; September-October 2022) season are shown for chlorophyll-*a* (chl_a) (a, 0-41 mg/L; d, 0-20 mg/L), temperature (Temp) (b, 18-23 °C; e, 24-32 °C) and dissolved oxygen (DO) (c & f, 150-250 µmol kg^{-1}) based on Environmental Protection Department (EPD) data measured at the sampling stations shown with green dots. Gradient flux (GF) instrument deployments (see Table 1) were undertaken to characterize community-scale NEP at three sites: (g) Tung Ping Chau (purple star), (h) Sharp Island (red star), and (i) Sham Wan (blue star). At each site, conductivity-temperature-depth (CTD) casts were undertaken along a transect denoted by the white circles. Satellite images in g-i derived from (Imagery © 2023 NASA, Map data © 2023 Google).

Coral ecosystems in eastern Hong Kong have high species diversity and abundance and are less affected by Pearl River discharge (Goodkin et al., 2011). Tung Ping Chau is especially isolated from the rest of Hong Kong, lying 10 km from the Hong Kong coast in Mirs Bay. While the waters surrounding Tung Ping Chau have previously been reported to have among the highest coverage and diversity of hard corals in Hong Kong (Xie et al., 2020), our surveys showed less coral cover around our deployment at Tung Ping Chau than at Sharp Island (see Results 3.1.5). However, Sharp Island in the past has shown evidence of higher bleaching rates than other sites in Hong Kong (Xie et al., 2020). During our deployments, outside peak summer conditions, there were no signs of significant bleaching affecting the community, likely due to rapid recovery of corals that bleached in August 2022, leading to near full recovery within months (Chung et al., 2024). The south of Hong Kong lies in the transitional zone where coral assemblages are still sporadically present, but abundances are limited by the impact of the Pearl River discharge (Duprey et al., 2016). Sham Wan, which is located in the middle of this transition zone and dominated

by rocky substrate (Yeung et al., 2021), was selected to represent the westernmost extent at which coral communities persist in Hong Kong.

The location of instrument deployments within sites were chosen based on visual inspection of the benthos by SCUBA divers such that the deployments were surrounded by relatively uniform coral communities on all sides that were roughly representative of the broader sites' composition. A summary of deployment parameters is available in Table 1. Changes in flow direction will lead to metabolism data being generated from different areas of benthic communities. Therefore, in this study, we selected deployment sites that were well surrounded, on all sides, by benthic cover as uniform as possible to account for unpredictable flow patterns.

Table 1. Summary of deployments during the dry (2021) and wet (2022) seasons showing the location, season, deployment dates, the mean and range in depth of deployment (in m), deployment duration (in days), and mean (± SEM.) net ecosystem production (NEP) value for each deployment.

Season	***Location***	***Dates***	***Depth (m)***	***Duration (days)***	***NEP_{mean} ($mmol\ O_2\ m^{-2}\ hr^{-1}$)***
Dry	*Sham Wan*	*23–30 Dec 2021*	*5.8 (4.7-6.7)*	*7*	*-0.37 ± 1.3*
	Sharp Island	*19–26 Nov 2021*	*3.3 (2.4-4.3)*	*7*	*0.12 ± 1.3*
	Tung Ping Chau	*30 Nov – 7 Dec 2021*	*3.8 (2.7-5.2)*	*8*	*-0.22 ± 0.9*
Wet	*Sham Wan*	*28 Oct – 11 Nov 2022*	*5.7 (4.5-6.8)*	*14*	*-0.37 ± 0.6*
	Sharp Island (May)	*18–24 May 2022*	*3.7 (2.7-4.9)*	*6*	*-1.39 ± 3.0*
	Sharp Island (Oct)	*29 Sept – 6 Oct 2022*	*3.6 (2.7-4.6)*	*7*	*0.15 ± 9.4*
	Tung Ping Chau	*11–21 Oct 2022*	*2.8 (2.0-3.6)*	*11*	*-0.59 ± 2.3*

To encompass major seasonal variations, deployments were carried out at each site during the dry season (November-December 2021) and at the end of the prolonged wet season in 2022 (October 2022; Table 1). An additional deployment was

completed earlier in the wet season (May 2022) at Sharp Island. Although October often marks the transition period between wet and dry season conditions, the October 2022 deployments were classified as wet season because Hong Kong temperatures remained elevated during this period. Specifically, Hong Kong experienced its hottest autumn on record in 2022, with a mean air temperature of 26.4 °C from September to November (Hong Kong Observatory, 2022). Furthermore, the mean water temperature measured during our October 2022 deployments (25.89 ± 2.13 °C) was characteristic of the long-term (1991-2020) average wet season (April-October) sea surface temperature values recorded by the Hong Kong Observatory (HKO) (https://www.hko.gov.hk/en/cis/normal/1991_2020.htm, Table 9, Waglan Island 1400 or 1700 hours) of 26.09 ± 2.02 °C, in contrast to the long-term average dry season (November-March) sea surface temperature of 19.58 ± 2.65 °C. We therefore refer to these as late wet-season deployments due to the elevated water temperatures extending into our deployment periods.

2.2 Water quality data and atmospheric conditions of Hong Kong

The environmental gradient around Hong Kong was characterized using periodic monitoring data collected by the Environmental Protection Department (EPD, https://cd.epic.epd.gov.hk/EPICRIVER/marine/?lang=en, date accessed 15 December 2023), focusing on the monthly data from the wet (September, October 2022) and dry season (December 2021, January 2022), closest to our deployment dates (Figure 1a-f). Surface-water data collected at 1 m depth was used because it best reflects the environmental conditions experienced by local coral communities due to their typically shallow distribution (1-6 m, Goodkin et al., 2011). For monitoring sites with multiple days of observations during the period of interest, values were averaged to give one seasonal value per station. The variables examined included dissolved oxygen (DO), turbidity, chlorophyll-*a* (chl *a*), temperature, and salinity. DO was converted from mg L^{-1} to µmol kg^{-1} for consistency in DO units used in this study. A constant density value of 1021.08 kg m^{-3}, the mean density value of the conductivity-temperature-depth (CTD) casts, was used for this conversion. Using this density value was necessary for unit conversion due to pressure not being provided in the EPD dataset. Standard error of the mean (SE) was reported instead of standard deviation (SD) with the means of the EPD data to better show variability across seasons. The examined variables were selected due to their ecological relevance to coral reef metabolic processes (Ferrier-Pages et al., 1999; Sawall et al., 2011; Long et al., 2013; Bessell-Browne et al., 2017; Nelson and Altieri, 2019) and availability across both seasonal periods during the deployments. Because EPD monitoring data are collected at monthly resolution, these values are used to characterize broad spatial and seasonal environmental context rather than the exact conditions experienced during each of the short-term deployments.

Atmospheric weather conditions were provided by the HKO (date received 22 December 2022) for the period of 2013 through 2022. Atmospheric variables used in the analysis were global solar radiation (MJ m^{-2} h^{-1}), wind speed (m s^{-1}) and rainfall (mm) due to their applicability in interpreting benthic light (Roth, 2014; Hochberg et al., 2024), turbidity (Riegl and Branch, 1995; Browne et al., 2014), salinity (Coles and Jokiel, 2018; Moberg et al., 1997; Manzello and Lirman, 2003) and mixing of the water column (Dennison and Barnes, 1988; van Hoytema et al., 2016), respectively. Each of these factors could impact measured NEP and can help explain seasonal differences.

2.3 Benthic community composition

The benthic community composition of the study sites, including substrate composition and the cover for each coral genus, was characterized based on underwater video surveys conducted at each site from September–October 2022. The surveys used a GoPro Hero4 Black camera to capture video transects based on a timed (5 min) swim by a roving diver, moving in a spiral motion outward and away from the deployed gradient flux (GF) system. Benthic analysis was undertaken using CoralNet (Beijbom et al., 2015). Photo quadrats were extracted from each video transect at approximately 10 second intervals. Due to poor quality (i.e., too blurry) of a few extracted images, we eventually were only able to obtain 28, 28, and 25 usable photo quadrats for Tung Ping Chau, Sharp Island, and Sham Wan, respectively. From each extracted photo quadrat, 100 random points were overlaid on each image with an annotation area set to exclude 20 % of the area from the peripheral to ensure no overlap between images. Major biotic and abiotic benthic groups (sand, rock, rubble) were annotated, and hard corals were identified to a finer genus level with notes on their health status (i.e., live and dead) when possible. Artificial items and unidentifiable or unknown objects were labelled as "Others-Abiotic" and "Unknown/Unidentifiable", respectively. Benthic community composition was presented as percent cover (%) for each benthic category. Macroalgae and turf algae were included as groups as well, but no significant coverage was identified for record at any of our sites. This finding is supported by past benthic studies completed in Hong Kong that showed algal abundance peaking during early Spring months and decreased substantially during the summer and early winter months (Yeung et al., 2021; Cheung-Wong et al., 2022).

2.4 Coral community metabolism measurement: gradient flux approach

To characterize the metabolic rates of Hong Kong coral communities, we collected autonomous measurements of benthic metabolism at high temporal frequencies (minutes) using a GF approach, which tracks chemical and velocity gradients in the benthic boundary layer to estimate benthic metabolic rates (McGillis et al., 2011). The GF technique has been used to assess NEP (McGillis et al., 2011; Turk et al., 2015; Takeshita et al., 2016; Coogan et al., 2022) on natural coral reefs, and at coral restoration sites (Platz et al., 2020). The GF approach relies on estimates of the mean chemical flux of DO from the benthic boundary layer to calculate NEP. In this study, the GF instrumentation consisted of two DO sensors (MiniDOT, Precision Measurement Engineering (PME), Vista, California, USA) and two velocimeters (Vector, Nortek, Norway) positioned at two heights above the benthos, z_1 and z_2. The lower height (Z_2) was positioned 8 cm above the substrate, and the top height (Z_1) was 124 cm above the substrate. It should be noted that our lower height (8 cm) was positioned closer to the substrate than previous GF studies (i.e., 10 cm (Pisapia et al., 2019); 20 cm (McGillis et al., 2011; Boles et al., 2026); 30 cm (Takeshita et al., 2016)) because the coral canopy at our sites is relatively low and patchy compared to other study sites higher-relief, more complex canopy settings. Therefore, this height was selected to remain within the benthic boundary layer while also avoiding direct obstruction by the benthos. The two DO sensors (accuracy = ± 9.5 μmol kg^{-1}) were cross calibrated immediately after each deployment to correct for any offset between the two sensors that could impact the DO gradient and to minimize the

impact of the uncertainty associated with the sensor accuracy. Fluxes of DO (mmol m^{-2} h^{-1}) were calculated using Eq. (1) (McGillis et al., 2011; Platz et al., 2020):

$$J_{DO} = \rho u^{*} \kappa \left(\frac{DO_{z1} - DO_{z2}}{ln\left(\frac{z_1}{z_2}\right)} \right) \quad (1)$$

where ρ is the seawater density (kg m^{-3}), u^* is the friction velocity (m s^{-1}), κ is the Kármán constant (0.40). This value is widely used for turbulent boundary layers and is supported by observations from coastal and reef environments, where κ typically falls within 0.35–0.50 (e.g., Gross & Nowell, 1983). Although κ can vary with local roughness and wave–current interactions, its inclusion in the diffusivity term is linear; therefore, using κ = 0.40 is appropriate and provides a robust estimate for our sites. As above, z_1 and z_2 are the higher and lower observation heights (m), respectively. DO_{zx} is the chemical concentrations (µmol kg^{-1}) at the respective heights z_x (z_1 or z_2). The friction velocity was calculated using Eq. (2) as described in McGillis et al., (2011):

$$u^{*} = \kappa \left(\frac{U_{z1} - U_{z2}}{ln\left(\frac{z1}{z2}\right)} \right) \quad (2)$$

where U_z is the 3-axis water velocity at the respective sensor height (m s^{-1}).

Metabolic rates are proportional to these chemical fluxes (McGillis et al., 2011) and were calculated based on Eq. (3) as:

$$NEP = -(J_{DO}) \quad (3)$$

2.5 High frequency in-situ characterization of prevailing environmental conditions

The salinity (S) of the seawater was determined using a miniature CTD sensor (accuracy = ± 0.05 mS cm^{-1}, DEFI-CT, JFE Advantech, Tokyo, Japan) attached halfway between the two sensor heights on the GF frame. At each height, the respective velocimeter was used to measure, in addition to water velocity, the pressure (P) and temperature (T) of the seawater. Deployment settings for the Vectors were set to sample at a rate of 16 Hz with burst sampling interval of 60 seconds using an ENU (East North Up) coordinate system. These settings were maintained across all deployments. During each deployment, a photosynthetically active radiation (PAR) sensor (accuracy = ± 5 %, MiniPAR, PME, Vista, California, USA) was also deployed directly on the benthos next to the GF system to record incident light levels, far enough away to avoid shading by the instrument. All sensors collected one data point every 60 seconds and were averaged over 10 minutes for final data analysis.

We also measured the vertical structure of the water column, in terms of T (°C), S (ppt), DO (µmol kg^{-1}), and chl *a* (µg L^{-1}), along an onshore-offshore transect across each coral community using a RINKO-profiler CTD (ASTD102, JFE Advantech, Tokyo, Japan) set to process data in 0.1 m depth bins through the water column. Due to logistical constraints, casts were only performed during the wet season deployments. Ten casts were made per site with the exact location of each cast shown by the white dots in Fig 1g-i.

2.6 Data pre-treatment

Data was omitted when GF assumptions were not met. Firstly, data were omitted when the top sensor velocity was lower than the bottom sensor velocity, showing that there was no law-of-the-wall relationship between the substrate boundary layer and the overlying water column (Platz et al., 2020). Because GF estimates require sufficient turbulent mixing, periods of very low near-bed flow were excluded. Rather than applying a single fixed velocity cutoff across all deployments, we removed observations falling below the 10^{th} percentile of bottom-sensor velocity within each deployment. This deployment-specific threshold was selected to exclude the weakest-flow periods most likely to violate GF assumptions while accounting for differences in background flow among sites and seasons.

A non-steady state boundary layer unsuitable for GF analysis was indicated when the standard deviation of the 60-second DO measurements within each 10-minute averaged time period was in the top 10 % of the distribution (> 90^{th} percentile), determined for each deployment individually; data was discarded in such cases. To ensure confidence in velocity measurements, Vector velocities were omitted when the correlation of any individual beam was < 50 %. If > 10 % of the burst sample (more than 1 of the 10 samples in each burst) was omitted, then that burst sample was not included in the 10-minute average velocity values used for further analysis, similar to the filter methods used in Coogan et al., (2022). These data filtering steps are necessary to reduce artefactual flux measurements. The retained dataset represents only periods when all GF assumptions were met, not necessarily every condition experienced during the deployment.

The 10-minute average values were used to provide time series for all environmental variables. Approximately 54.47% of the dry season data and 62.94 % of the wet season data were removed with these filters applied, averaged for all deployments, omitting Sham Wan in the wet season, where 86.04 % of data were removed largely due to a malfunction of the bottom DO sensor making metabolism calculations impossible. Hourly-averaged NEP rates were used for plotting these time series. Any gaps in the time series are the result of either sensor failure due to water leakage or battery malfunction or, in the case of measurements of metabolism, violations of the conditions required for GF calculations described above. All calculations related to metabolism were performed in MATLAB (R2020b, The MathWorks Inc, Natick, Massachusetts, USA).

2.7 Statistical analyses

To assess spatial and diel variation in community metabolism, we conducted non-parametric statistical tests on NEP for each deployment. Analyses were performed separately for the dry season and wet season datasets. Timestamps were categorized into “Day” (7am-6pm) and “Night” (6pm-7am). Mean values were computed separately for each time category at each site. To test for significant differences in NEP between Day and Night, we applied the Mann–Whitney U test for each site individually. A Bonferroni correction was used to adjust for multiple pairwise comparisons ($\alpha = 0.05$). For deployments with valid data in both diel periods, the Mann–Whitney U statistic, raw p-value, and Bonferroni-adjusted p-value were calculated.

To identify the environmental variables most strongly associated with changes in NEP during each deployment, we quantified pairwise correlations between NEP and measured environmental parameters. Prior to this analysis, NEP values were

regressed against PAR to isolate the light-driven component of NEP variability that would otherwise obscure the relationship between PAR and other measured variables (Khrizman et al., 2025). For each deployment, a simple linear model of the form:

$$NEP_{expected} = \alpha \times PAR + C \quad (4)$$

where α is the photosynthetic efficiency coefficient determined through the slope of the NEP/PAR relationship, and C is the intercept at zero irradiance. The residuals of this model,

$$NEP_{residual} = NEP_{observed} - NEP_{expected} \quad (5)$$

represent the portion of NEP variability independent of irradiance. Pearson correlation coefficients (r) and associated p-values were then computed between both the original NEP and the light-removed NEP residuals and each environmental predictor variable (water velocity, temperature, depth and salinity). Only relationships that were statistically significant ($p < 0.05$) were retained for result reporting and discussion.

Because assumptions of normality and equal variance were not met for several variables in the extracted EPD dataset, we employed the Mann-Whitney U test to determine whether median values of each parameter differed significantly between seasons. A significance threshold of $p < 0.05$ was used to identify meaningful seasonal differences. Simple linear regression was used to determine the correlation between PAR measured in-situ and global solar radiation derived from HKO weather data to examine light attenuation at the benthos. Global solar radiation was converted from Mj m^{-2} hr^{-1} to PAR units of µmol m^{-2} s^{-1} for slope comparison using a two-step process. First, global solar radiation values were converted to irradiance in watts per square meter (W m^{-2}) by multiplying by 277.78, recognizing that 1 MJ m^{-2} h^{-1} equals 277.78 W m^{-2}. Subsequently, to approximate PAR, the irradiance values were multiplied by an empirical conversion factor of 2.02 µmol J^{-1}. This factor reflects the proportion of solar energy within the PAR spectrum (400–700 nm) and is consistent with values reported in previous studies (Wang et al., 2024). The complete conversion formula is as follows:

$$PAR = Global\ solar\ radiation\ x\ 561.1 \quad (6)$$

Data from the HKO were analyzed according to a targeted dataset corresponding to the instrument deployment periods in the dry season (November–March 2021) and wet season (April–October 2022). For each environmental variable, we parsed and combined all relevant stations that measured a variable of interest (Light: Sai Kung; Wind speed; Sai Kung, Ping Chau and Lamma Island; Rainfall: Sai Kung, Ping Chau and Lamma Island). Values were grouped into wet season (April–October) and dry season (November–March) for the long-term dataset. For the deployment-time-specific dataset, seasonal grouping followed calendar year (i.e., dry = 2021; wet = 2022). We calculated seasonal means, standard deviations (± SD), and ranges for each variable. To test significant differences between wet and dry seasons within each dataset, we first assessed the normality of the data using the Shapiro-Wilk test. All variables were found to deviate significantly from a normal distribution ($p < 0.05$), so non-parametric Mann-Whitney U tests were used to compare medians between seasons. Kruskal-Wallis and

associated post-hoc Dunn's tests were used to test for differences in weather variables between deployments within seasons as well.

3 Results

3.1 Environmental conditions

3.1.1 Characterization of the vertical biophysical profile across sites

CTD casts measuring the range and mean (± SD) temperature, DO, and chl *a* were completed in October 2022 to assess the vertical water column structure at each site (Fig 2). DO stratification is reported as the average difference in DO (ΔDO) between the top and bottom cast from each deployment. Temperature along the Tung Ping Chau transect was spatially uniform (Fig 2b), averaging 28.0 ± 0.1 °C (range = 27.9-28.3 °C) with minimal vertical stratification ($\Delta T = T_{surface} - T_{bottom} = 0.18$ °C). DO concentrations were similarly homogeneous (mean = 173.7 ± 2.8 μmol kg^{-1}; range = 167.7-181.8 μmol kg^{-1}) with weak stratification (ΔDO = −5.45 ± 1.92 μmol kg^{-1}) (Fig 2c). Chl *a* concentrations were low to moderate (mean = 0.79 ± 0.28 μg L^{-1}; range = 0.35-1.42 μg L^{-1}) and exhibited weak vertical gradients (Fig 2a), indicating well-mixed, oxygenated conditions across the CTD transect. The narrow temperature and DO ranges observed in the contour plots support limited water-column stratification and low variability with distance from shore. Sharp Island displayed the greatest vertical and spatial variability among the three sites. Temperatures averaged 29.2 ± 0.4 °C (range = 28.7-29.8 °C) (Fig 2e) with a mean surface–bottom gradient of 0.8 °C, reflecting moderate thermal stratification. Dissolved oxygen varied substantially (Fig 2f), ranging from 69.45-183.53 μmol kg^{-1} (mean = 169.28 ± 22.60 μmol kg^{-1}) with strong stratification in DO (ΔDO = −81.53 ± 33.70 μmol kg^{-1}). The DO contour plot shows an oxygen minimum near the seabed in offshore casts. Chl *a* concentrations (mean = 0.79 ± 0.67 μg L^{-1}; range = 0.22-2.99 μg L^{-1}) (Fig 2d) increased offshore and at depth, aligning with enhanced stratification and possible subsurface productivity layers. Overall, the sharper vertical gradients at Sharp Island indicate stronger water column stability and low DO conditions in deeper water compared to the other sites.

At Sham Wan, temperature averaged 25.3 ± 0.9 °C (range = 24.0-26.8 °C) (Fig 2h) with modest vertical gradients ($\Delta T \approx 0.24$ °C). DO was slightly higher on average than at the other sites (mean = 153.03 ± 14.35 μmol kg^{-1}; range = 124.00-178.44 μmol kg^{-1}) (Fig 2i) and showed weak stratification (ΔDO = 6.16 ± 1.75 μmol kg^{-1}). Chl *a* concentrations were lower and more uniform (mean = 0.67 ± 0.37 μg L^{-1}; range = 0.06-1.48 μg L^{-1}) (Fig 2g), consistent with vertically mixed, well-flushed conditions within this semi-exposed embayment. The CTD transects highlight limited vertical structure and relatively high oxygenation throughout the water column, suggesting efficient turbulent exchange and minimal stratification.

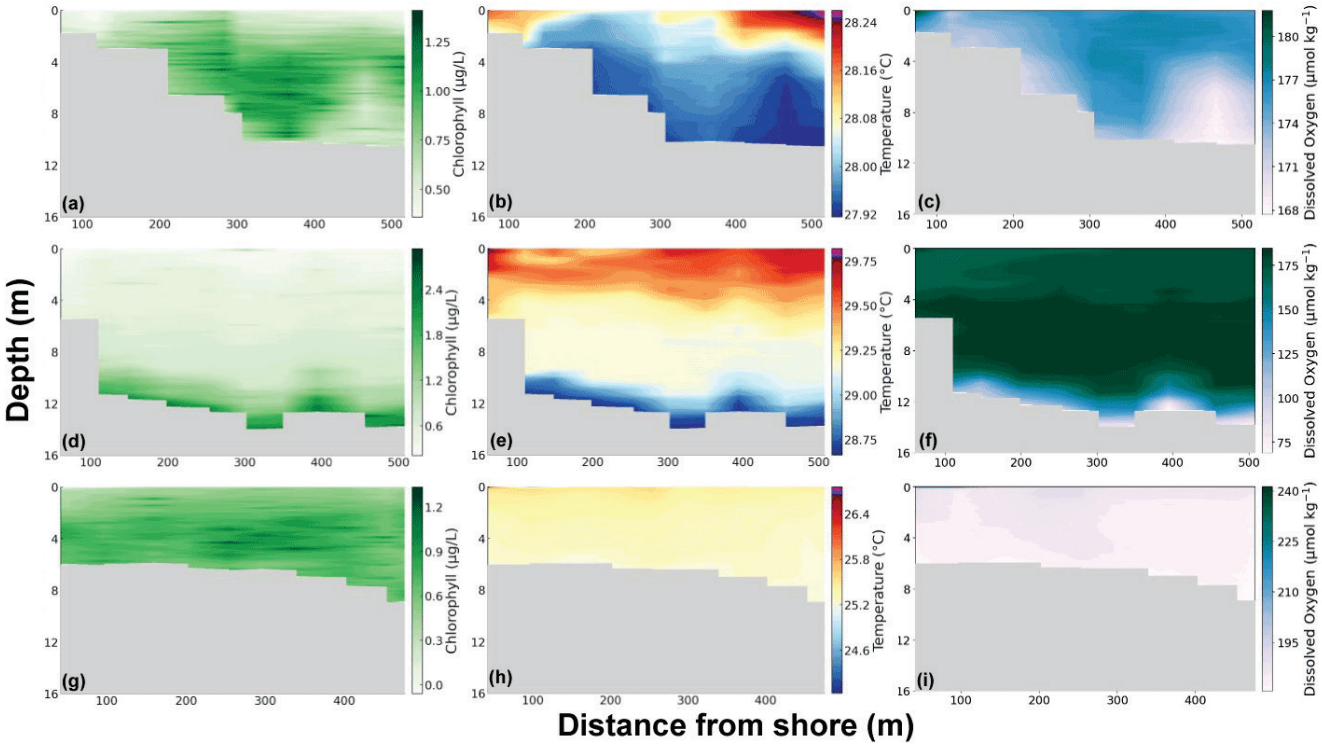

307

308 **Figure 2.** Vertical water column structure at each site. Contours show (a, d, g) Chlorophyll-*a* (Chl *a*) concentration (in µg L^{-1}), (b, e, h)
309 temperature (in °C), and (c, f, i) dissolved oxygen (DO) (in µmol kg^{-1}) based on CTD casts taken in October 2022 at each of the deployment
310 sites. Tung Ping Chau (row 1): (a) Chl *a*, (b) temperature, and (c) DO. Sharp Island (row 2): (d) Chl *a*, (e) temperature and (f) DO. Sham
311 Wan (row 3) (g) Chl *a*, (h) temperature, and (i) DO. The distance from shore of the CTD casts is shown on the x axis (in m).

312 **3.1.2 Seasonality in the environmental water quality gradient**

313 Based on EPD data collected during both deployment seasons (see Table S1 for full list of means (± SE) and ranges), the wet
314 season was less saline, more turbid, and displayed higher temperatures and lower DO than the dry season. Mann-Whitney U-
315 tests revealed significant differences in the medians between seasons of each variable tested ($p < 0.05$), except for chl *a* ($p =$
316 0.079; Table S1). The wet season (Figure 1d, e, f) exhibited highly variable turbidity, with a mean value (± SEM) of 27.9 ±
317 4.3 NTU. Salinity had a wide range in the wet season (17.5-33.9 psu) and lower DO (mean = 165.9 ± 1.8 µmol kg^{-1}).
318 Temperatures averaged 28.4 ± 0.11 °C during the wet season.

319 The dry season (Figure 1a, b, c) displayed less turbid, more saline water, lower temperatures, and higher DO compared
320 to the wet season. Dry season turbidity had a mean value of 19.3 ± 2.1 NTU. Salinity values ranged from 18.8 to 34.4 psu. DO
321 had a mean value of 197.3 ± 1.8 µmol kg^{-1}. Temperature dropped to a mean value of 22.6 ± 0.14 °C during the dry season.

3.1.3 Atmospheric weather conditions

During the deployment periods, weather data similarly showed significant differences between wet and dry seasons for solar radiation and wind speed. Solar radiation was higher in the wet season (1.02 ± 1.05 MJ m^{-2} h^{-1}) than in the dry season (0.86 ± 0.91 MJ m^{-2} h^{-1}; U = 2.31 × 10^5, p = 0.0052). Wind speed was significantly greater during the wet season (4.10 ± 2.67 m·s^{-1}) compared to the dry season (3.02 ± 2.10 m s^{-1}; U = 6.69 × 10^5, p < 0.001). While rainfall did not differ significantly between seasons during the specific date ranges where GF deployments were being completed (wet: 0.11 ± 0.93 mm h^{-1}; dry: 0.02 ± 0.16 mm h^{-1}; U = 5.04 × 10^5, p = 0.696), rainfall was significantly different between seasons when assessed over the entire seasonal timescale (Dry season = November 2021-March 2022, Wet season = April 2022-October 2022), with a mean (± SD) rainfall in the dry season of 0.068 ± 0.482 mm h^{-1} versus 0.329 ± 1.999 mm h^{-1} in the wet season (U = 7.9 × 10^7, p = 2.39 × 10^{-37}).

Weather data were also significantly different between deployment times within seasons as well. In the dry season, global solar radiation, wind speed, and rainfall were all significantly different between the Tung Ping Chau and Sham Wan deployment (p = 0.0058, Table S2). The dry season Sharp Island deployment had significantly different wind speed and rainfall compared to Tung Ping Chau and Sham Wan, respectively. During the wet season, Tung Ping Chau and Sham Wan deployments had significantly different global solar radiation and rainfall. Additionally, Sharp Island's wind speed differed from Tung Ping Chau, and the rainfall differed compared to during the Sham Wan deployment (p = 0.0043, Table S2).

3.1.4 In-situ environmental conditions

Environmental conditions differed significantly (Man-Whitney U test, p < 0.001) between seasons when averaged across all sites. The wet season (Figure 3g-l) had significantly higher average daytime PAR (194.21 ± 100.23 µmol m^{-2} s^{-1}) and average water temperature (25.89 ± 2.13 °C) compared to the dry season (55.53 ± 34.81 µmol m^{-2} s^{-1}, 21.88 ± 1.27 °C) (Figure 3a-f). DO and salinity were significantly lower in the wet season (181.76 ± 27.35 µmol kg^{-1}, 32.77 ± 0.59 ppt) compared to the dry season (202.25 ± 14.62 µmol kg^{-1}, 33.72 ± 0.27 ppt). The direction of the dominant water flow remained constant from dry to wet season at all three sites. (Figure S1). Sharp Island displayed the most extreme values for many of the environmental variables recorded; in the wet season it had the highest mean water temperature (28 °C), lowest mean DO (165 µmol kg^{-1}), and lowest salinity (32.1 ppt), indicating more extreme conditions at the site over and above seasonal variations. Mean values and ranges for all environmental variables measured at each site and season can be found in Supplementary Information (Table S3, Table S4).

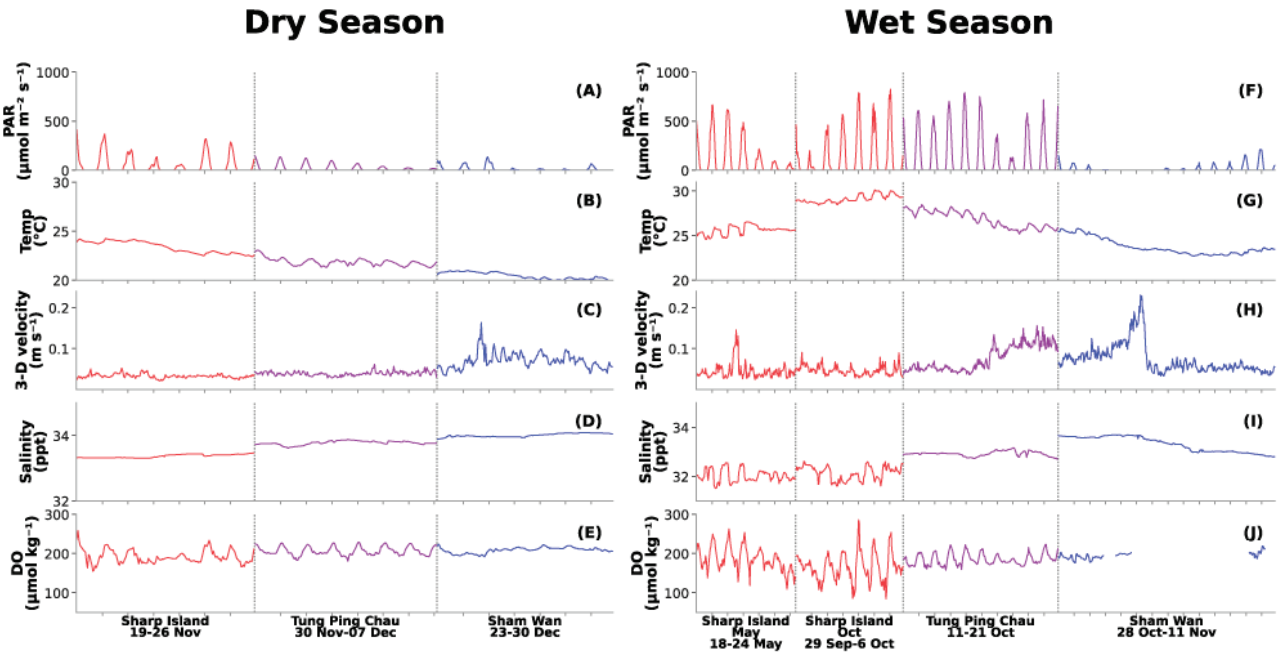

Figure 3. Comparison of prevailing environmental conditions measured during each deployment in the (a-e) dry and (f-j) wet seasons. Panels show photosynthetically active radiation (PAR) (µmol m^{-2} s^{-1}; a, f), temperature (temp) (°C; b, g), 3-dimentional water velocity (3-D velocity) (m s^{-1}; c, h), salinity (ppt; d, i), and dissolved oxygen (DO) (µmol kg^{-1}; e, j) for Tung Ping Chau (purple lines), Sharp Island (red lines) and Sham Wan (blue lines).

3.1.5 Benthic community composition

The estimated benthic community compositions are shown in Table 2. Focusing on major components of the benthic substrate (> 1 %), Tung Ping Chau was dominated by rock/rubble (38.89 ± 24.34 %), live coral (36.14 ± 29.59 %), sand (21.14 ± 16.75 %), and dead coral (4.36 ± 7.71 %). The dominant coral genera present (reported as percent of total benthic cover) were *Porites* (2.89 ± 6.75 %), *Acropora* (8.04 ± 17.52 %), and *Platygyra* (23.86 ± 21.26 %). At Sharp Island, the substrate was predominately composed of live coral (65.75 ± 22.84%), with sand (18.14 ± 14.01 %), rock/rubble (10.71 ± 8.26%), and dead coral (3.66 ± 4.05 %). Within the live coral cover, *Acropora* (46.46 ± 25.99 %), *Pavona* (17.32 ± 21.25 %) and *Porites* (1.36 ± 3.08%) dominated the site. At Sham Wan, the benthos was mainly rock/rubble (59.4 ± 24.82 %) and sand (36.6 ± 26.16 %), with only a small amount of live coral (3.84 ± 7.37 %). The only coral species observed in any numbers here was *Plesiastrea* (2.72 ± 7.37 %). Its very low coral cover and dominance of rocky substrate support prior studies that show that Sham Wan is close to the westernmost extent of coral cover in Hong Kong, providing contrast with the higher coral cover communities at Tung Ping Chau and Sharp Island.

Table 2. Benthic community composition around the deployment locations at Tung Ping Chau, Sharp Island and Sham Wan as percentage total benthic cover. Tung Ping Chau's live coral cover was dominated by *Platygyra* while Sharp Island was dominated by *Acropora*. Corals were largely absent from Sham Wan, which was dominated by rock/rubble and sand.

	***Acropora* (%)**	***Pavona* (%)**	***Porites* (%)**	***Platygyra* (%)**	***Plesiastrea* (%)**	**Sand (%)**	**Rock/Rubble (%)**	**Live Coral (%)**	**Dead coral (%)**
Tung Ping Chau	8.04 ± 17.52	0.00 ± 1.50	2.89 ± 6.75	23.86 ± 21.26	0.00 ± 0.00	21.14 ± 16.75	38.89 ± 24.34	36.14 ± 29.59	4.36 ± 7.71
Sharp Island	46.46 ± 25.99	17.32 ± 21.25	1.36 ± 3.08	0.00 ± 2.60	0.00 ± 0.00	18.14 ± 14.01	10.71 ± 8.26	65.75 ± 22.84	3.66 ± 4.05
Sham Wan	0.00 ± 0.00	0.00 ± 0.00	0.00 ± 0.00	0.00 ± 0.00	2.72 ± 7.37	36.60 ± 26.16	59.40 ± 24.82	3.84 ± 7.37	0.00 ± 0.00

3.2 Benthic community metabolic rates

3.2.1 Dry season

Significant spatial and diel variability in NEP was detected during the dry season (Figure S2), with Tung Ping Chau and Sham Wan displaying net respiration (negative NEP) and Sharp Island NEP being slightly net productive (positive NEP). Diel comparisons of NEP within each site revealed significant differences between day and night (Figure 4a-c). Mann–Whitney U tests yielded statistically significant contrasts at Sharp Island ($p < 0.001$, daytime NEP = 0.31 ± 1.47 mmol O_2 m^{-2} hr^{-1}, nighttime NEP = -0.31 ± 0.44 mmol O_2 m^{-2} hr^{-1}) and Tung Ping Chau ($p < 0.001$, daytime NEP = 0.15 ± 0.87 mmol O_2 m^{-2} hr^{-1}, nighttime NEP = –0.69 ± 0.72 mmol O_2 m^{-2} hr^{-1}), indicating a shift from net production to net respiration over the diel cycle. Sham Wan did not show significant differences between day and night NEP ($p = 0.176$, daytime NEP = –0.40 ± 0.36 mmol O_2 m^{-2} hr^{-1}, nighttime NEP = –0.34 ± 0.30 mmol O_2 m^{-2} hr^{-1}).

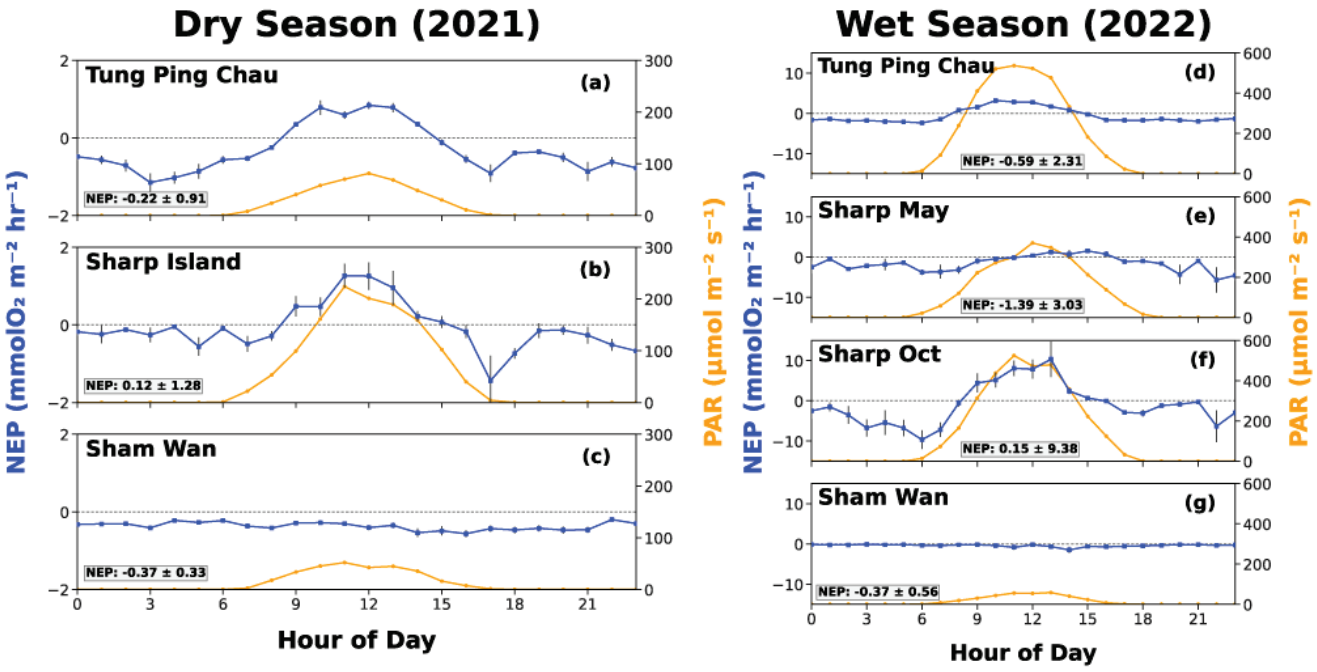

382

383 **Figure 4.** Diel composite plots of hourly averaged net ecosystem production (NEP) (blue line) and photosynthetically active radiation (PAR)
384 (orange line) for the dry season (a-c) and wet season (d-g) deployments. Error bars represent ± standard error of the mean NEP for each
385 hourly bin. Text boxes show the mean ± SD NEP (mmol O_2 m^{-2} hr^{-1}). Note the expanded NEP and PAR axis ranges for the wet season
386 figures relative to the dry season to capture the larger variability observed during the wet season.

387 **3.2.2 Wet Season**

388 In the wet season, all sites were net respiring except for Sharp Island in October which was slightly net productive. NEP also
389 exhibited significant diel variation across all deployments (Figure S3). Mann–Whitney U tests revealed consistent and
390 significant differences in NEP ($p < 0.001$) between day and night at all sites (Figure 4d-g). Tung Ping Chau NEP (daytime =
391 0.77 ± 2.48 mmol O_2 m^{-2} hr^{-1}, nighttime = –1.78 ± 1.28 mmol O_2 m^{-2} hr^{-1}) and Sharp Island NEP in both May (daytime = –
392 0.63 ± 2.85 mmol O_2 m^{-2} hr^{-1}, nighttime = –2.65 ± 1.35 mmol O_2 m^{-2} hr^{-1}) and October (daytime = 2.10 ± 9.67 mmol O_2 m^{-2}
393 hr^{-1}, nighttime = –1.78 ± 1.28 mmol O_2 m^{-2} hr^{-1}) was significantly greater during the day than at night. Sham Wan NEP was
394 significantly lower ($p = 0.0051$) during the day (–0.53 ± 0.80 mmol O_2 m^{-2} hr^{-1}) versus the night (–0.27 ± 0.28 mmol O_2 m^{-2}
395 hr^{-1}).

396 **3.3 Environmental drivers of NEP**

397 **3.3.1 Dry season**

398 At Sharp Island, NEP (Figure S4**)** was strongly correlated with PAR ($r = 0.57$, $p < 0.001$), while weak negative correlations
399 were also observed with bottom depth ($r = −0.16$, $p = 0.01$) and salinity ($r = −0.14$, $p = 0.026$). After removal of the PAR

effect, none of these variables remained significantly correlated with the NEP residuals, indicating that NEP variability at this site was almost entirely governed by light availability.

At Tung Ping Chau, NEP also showed a significant positive correlation with PAR ($r = 0.61$, $p < 0.001$), while no other environmental parameters displayed significant relationships with either NEP or NEP residual. This suggests that community metabolism at Tung Ping Chau during the dry season was tightly coupled to irradiance and largely insensitive to variation in flow, temperature, or salinity.

In contrast, Sham Wan exhibited a broader range of significant relationships. NEP was positively correlated with bottom velocity ($r = 0.14$, $p = 0.002$), negatively correlated with bottom temperature ($r = -0.22$, $p < 0.001$), and positively correlated with salinity ($r = 0.12$, $p = 0.005$). These same variables remained significant after removing the PAR effect, with NEP residuals correlated with velocity ($r = 0.14$, $p = 0.001$), temperature ($r = -0.23$, $p < 0.001$), and salinity ($r = 0.13$, $p = 0.004$). This persistence of correlations in the light-removed dataset indicates that hydrodynamic and thermal processes exerted independent control on community metabolism at Sham Wan.

3.3.2 Wet season

At Sharp Island in May (Figure S5), NEP was significantly correlated with PAR ($r = 0.53$, $p < 0.001$) and water velocity ($r = 0.24$, $p < 0.001$). After removal of the PAR effect, NEP residuals remained significantly correlated with velocity ($r = 0.17$, $p = 0.014$), temperature ($r = 0.24$, $p < 0.001$), and salinity ($r = -0.16$, $p = 0.020$), indicating additional light-independent influences on benthic organic metabolism during this deployment.

In October at Sharp Island, NEP was strongly correlated with PAR ($r = 0.63$, $p < 0.001$), as well as temperature ($r = 0.32$, $p < 0.001$), depth ($r = -0.36$, $p < 0.001$), and salinity ($r = -0.11$, $p = 0.045$). However, none of these secondary correlations persisted in the NEP residuals, demonstrating that NEP variability was primarily driven by light and diurnally covarying thermal and hydrographic changes.

At Tung Ping Chau, NEP exhibited a very strong relationship with PAR ($r = 0.72$, $p < 0.001$) and a weaker positive correlation with velocity ($r = 0.09$, $p = 0.009$). These relationships disappeared for the NEP residuals, suggesting that short-term fluctuations in flow and temperature were largely covariant with light availability.

In contrast, Sham Wan showed significant correlations of NEP with PAR ($r = 0.41$, $p < 0.001$), bottom velocity ($r = 0.12$, $p = 0.006$), and bottom temperature ($r = -0.22$, $p < 0.001$). The NEP residuals remained significantly related to both velocity ($r = 0.11$, $p = 0.012$) and temperature ($r = -0.20$, $p < 0.001$).

4 Discussion

A growing number of studies have focused on measuring community-scale NEP over coral assemblages, utilizing primarily autonomous methods (Takeshita et al., 2018; Platz et al., 2022). To our knowledge, this is the first study assessing high-resolution, in-situ NEP and associated organic carbon cycling over coral communities in a marginal, highly urbanized

environment. The three study sites occur within the broader marginal environmental setting of Hong Kong, but differ in benthic structure and coral cover. Sham Wan showed clear structural marginality, with very low coral cover and dominance of rocky substrate, whereas Sharp Island and Tung Ping Chau maintained moderate to high coral cover. Across these contrasting benthic settings, however, all sites showed low or negative short-term NEP, indicating constrained community-scale net organic carbon production during deployment periods. We therefore interpret NEP not as a complete measure of reef function or health, but as a measure of one important component of ecosystem function: the balance between photosynthesis and respiration (Brandl et al., 2019; Schoepf et al., 2023). Quantifying how this component of organic carbon cycling varies across Hong Kong's environmental gradient can help clarify how coral communities persist under local stressors and changing ocean conditions, including coastal urbanization and global change. The spatiotemporal patterns in NEP quantified here therefore provide a basis for identifying natural background variability in community carbon cycling and for assessing how communities may change under future ocean conditions.

The low and generally negative NEP observed in Hong Kong coral communities in this study adds to a growing number of studies that challenge the notion that coral ecosystems are by default highly net productive environments (Odum and Odum, 1955; Gattuso et al., 1996). Corals are the predominant contributor to community productivity, especially in environments like our study sites where algal abundance is low. When these corals shift their metabolic balance to heterotrophic feeding rather than a dependence on photosynthetic sources, as has been shown to happen in turbid reefs (Travaglione et al., 2023), the community-scale cumulative respiration signal of the corals and other respiring organisms found in high abundance in these communities in Hong Kong, such as reef fishes (especially in high coral cover sites, Yiu et al., 2025) and sea urchins (Dumont et al., 2013; Qiu et al., 2014), may outweigh, or occur alongside suppressed, autotrophic production. Interestingly, the high abundance of urchins found within Hong Kong coral communities has also been shown to be a leading cause of low algal abundance through grazing (Suarez et al., 2021), in addition to seasonality related decreases in algal populations (Yeung et al, 2021). It should also be noted that community-scale net respiration is not exclusive to turbid environments. A growing number of studies conducted in more pristine reef environments have also reported net community respiration (Kaneohe Bay, Hawaii; Falter et al., 2008, Shamberger et al., 2011; Cheeca Rocks, Florida and La Parguera, Puerto Rico; Melendez et al., 2022; Chagos Archipelago; Khrizman et al., 2025; Palmyra atoll; Takeshita et al., 2016; Florida Keys; Coogan et al., 2022). Longer timescale studies investigating organic metabolism over a wide range of coral habitats are needed to better elucidate what local factors are driving observed shifts in metabolic balance over space and time.

4.1 Spatiotemporal patterns in NEP

4.1.1 Identifying possible drivers of suppressed productivity in Hong Kong coral communities despite high coral cover

Our results support that coral cover alone may not be a reliable indicator of contemporary community-scale organic carbon production in coral communities (Page et al., 2017), and that persistence of these communities in marginal environmental

settings may depend on mechanisms such as heterotrophic subsidies, stress-tolerant taxa, low macroalgal competition, and recovery from episodic disturbances rather than consistently high net autotrophy.

Although low light availability emerged as the dominant measured driver of NEP in this study, we interpret this as one mechanism driving the observed low NEP rather than the sole defining characteristic of the system. Low light suppresses autotrophic production of the communities, but several other possible mechanisms may be acting to increase respiration rates in these communities as well. Excessive eutrophication has been shown to be the dominant control over modern-day coral community composition in Hong Kong (Cybulski et al., 2020; Duprey et al., 2020). Elevated allochthonous nutrient inputs into coral environments have been shown to have mixed effects on coral NEP (D'Angelo and Wiedenmann, 2014; Silbiger et al., 2018; Barnas et al., 2025); however, the beneficial aspects of elevated nutrients in increasing NEP largely are derived from increased production rates with adequate light levels to support it. This is not the case in this study in Hong Kong, where the light-limiting environment appears to suppress the positive effects of nutrients loads to NEP. In contrast, external nutrient input will increase sediment and microbial respiration (Kelly et al., 2014; Silbiger et al., 2018) and, perhaps most crucially, increase nighttime respiration rates of the coral community when no photosynthesis is occurring (Falter et al., 2011; Long et al., 2013). Therefore, when evaluating the impact that chronic eutrophication of Hong Kong coastal waters has on community organic cycling, it is likely that it enhances respiration rates at a greater rate than any positive effect it has on enhancing photosynthesis rates. The combined effects of low-light limitation on photosynthesis production and increased respiration rates driven by excess nutrient loads potentially act together to suppress NEP rates of coral communities in Hong Kong, compared to tropical oligotrophic reef counterparts.

4.1.2 Seasonality in NEP

All of our deployments, across sites and seasons, indicated that these communities are net respiring or only slightly net productive, with average net respiration rates (-NEP) ranging from -1.39 ± 3.03 to 0.15 ± 9.38 mmol O_2 m^{-2} hr^{-1}. This suggests that the coral communities across Hong Kong are limited in their photosynthetic capacity, or that respiring organisms' metabolic rates exceeds rates of photosynthesis. PAR was shown to be a consistent primary driver of NEP rates during this study, so prolonged periods of cloudy weather could have a serious effect on suppressing NEP in this region. Hong Kong generally experiences reduced light conditions compared to other coral rich environments around the world. Mean daily solar radiation during the deployment period was approximately 4.0 kWh m^{-2} day^{-1}, equivalent to 337 µmol m^{-2} s^{-1} when converted to PAR-equivalent units (Hong Kong Observatory 2025; Figure S6). By comparison, equivalent values were approximately 421-505 µmol m^{-2} s^{-1} on the Great Barrier Reef (SolCast Pty Ltd. 2025), 421-547 µmol m^{-2} s^{-1} in the Caribbean (NASA Langley Research Center 2025), and 505-589 µmol m^{-2} s^{-1} in the Red Sea (SolarGIS s.r.o. 2025). In combination with the strong net respiration signals seen during night hours in these coral communities (Daytime $NEP_{mean} = 0.42 \pm 4.21$ mmol O_2 m^{-2} hr^{-1} versus Nighttime $NEP_{mean} = -1.26 \pm 2.39$ mmol O_2 m^{-2} hr^{-1}), cloudy days and turbid water conditions will act in unison to suppress production rates. Despite the wet season displaying environmental conditions more conducive to positive NEP (higher PAR), these communities exhibit similarly low production year-round, regardless of season. A prior mesocosm study in Hong

Kong documented that low light contributes to limitation of productivity in these coral communities (McIlroy et al., 2019), along with limiting the distribution of coral assemblages (Cybulski et al., 2020; Yeung et al., 2021). This suggests that, unlike other reef communities where NEP is reduced during the winter, but elevated during summer (Falter et al., 2012; Stoltenberg et al., 2020), in Hong Kong it is negative year-round. This worrying trend may be enhanced in the future as an increase in cloud cover and a corresponding decrease in surface solar radiation have been observed in Hong Kong over the past decades (Hong Kong Observatory, 2022). It must be noted that attempts to fit a photosynthesis–irradiance (PI) relationship to the observed NEP data were unsuccessful, as NEP did not approach saturation with increasing PAR at any site. The absence of a discernible maximum NEP under light saturation (P_{max} (Takeshita et al., 2016)) suggests that the ambient light regime in these Hong Kong coral communities remained below saturating levels for photosynthesis throughout the study period. This pattern is consistent with chronic light limitation, likely driven by high turbidity that has been shown to limit community productivity in other light-limited environments (Law and Huang, 2023).

Greater magnitude and more variable net respiration was evident in the wet season (NEP_{mean} = –0.49 ± 4.83 mmol O_2 m^{-2} hr^{-1}) compared to the dry season (NEP_{mean} = –0.21 ± 0.85 mmol O_2 m^{-2} hr^{-1}). This suggests that seasonal environmental changes in the wet season may enhance respiration rates at a greater pace than increasing production, despite higher PAR in the wet season that may increase photosynthesis. One of these seasonal changes that could lower NEP in the wet season is lower salinity. Lower salinity in the wet season (Table S3, Table S4) driven by higher rainfall has been shown to induce physiological stress on coral communities in Hong Kong (Xie et al., 2020), possibly reducing their ability to maintain higher productivity. DO was also lower during the wet season, which could have decreased NEP values as well; however, low oxygen conditions have been shown to inhibit both photosynthesis and respiration of corals (Nelson and Altieri, 2019), so further studies investigating the role of low DO conditions on NEP rates over more coral habitats are needed. Finally, higher water temperatures during the wet season likely increased respiration rates of corals (Parry et al., 2025), and other respiring organisms (Nilsson et al., 2010; Tran and Johansen, 2023), in the community, further decreasing NEP in the wet season versus the dry season.

Weather patterns could also have had a role in changing community-scale organic carbon cycling. Specifically, higher rainfall in the wet season could also have contributed to the lower and more variable NEP values. While rainfall did not significantly differ during the specific short-term deployment periods between seasons, rainfall was significantly higher during the wet season than the dry season when averaged over the entire season (Wet; April-October 2022, Dry; November 2021-March 2022). Increased rainfall can lead to several changes in the local environment of the coral communities that could increase the variability in NEP, such as increased terrestrial runoff leading to increased organic matter input (Haapkylä et al., 2011) or increased stratification of the water column due to freshwater intrusion (Goodkin et al., 2011; Zhou et al., 2012). Future studies should investigate in more detail, utilizing in-situ sensors with increased temporal resolution, what factors influence the relative level of both chemical and physical stratification in the water column to better elucidate the impact rainfall or other sources of runoff may have on the strength of stratification. During periods of strong stratification, the GF may not be an appropriate method to measure NEP (Takeshita et al., 2016) due to the assumptions of the GF method being

violated and an overprediction of the respiration signal due to reduced vertical flux across the benthic boundary layer (Coogan et al., 2022).

The effect of the temperature gradient on NEP rates was monitored and assessed to account for this possible methodological artefact in our dataset. The strength of temperature stratification varied spatiotemporally between sites and seasons (Figure S7, Figure S8) but did not exceed 0.5°C at any time during the deployment; therefore, it was not considered to significantly affect the metabolism measurements of this study. However, we recommend future studies utilizing the GF technique in strongly stratified waters measure the salinity at both the top and bottom depth to better account for the influence of stratification on metabolism measurements.

The GF method also cannot be used during periods of intense water column mixing due to the lack of a steady state boundary layer and the deterioration of the law-of-the-wall relationship in the velocity profile with respect to the substrate. An illustration of this in our dataset was during the wet season Tung Ping Chau deployment: on 17 October 2022, Typhoon Nesat impacted Hong Kong coastal waters, causing intense water mixing. Following this storm event, until the end of the deployment time (18-21 October 2022), NEP rates could not be calculated due to the water velocity at the bottom height (z_2 = 8 cm) being consistently greater than the velocity at the top height (z_1= 124 cm), violating an assumption necessary for GF NEP calculations. Accordingly, retained NEP estimates represent periods when GF assumptions were satisfied and should be interpreted as high-resolution estimates under suitable boundary-layer and flow conditions, rather than as continuous deployment-scale averages across all hydrodynamic states experienced by the communities. Future studies should include analysis of weather conditions during deployment periods to reveal periods where intense stratification or water column mixing may be occurring, especially studies done during seasons with increased storm frequency such as the wet season in Hong Kong (Hong Kong Observatory, 2025).

4.1.3 Spatial patterns in NEP

Sham Wan displayed the lowest diurnal and seasonal variability and ranges in NEP during our study. The minimal diurnal variation in NEP likely reflects the relatively low density of metabolically active benthic organisms at this rock-dominated site (Figure 4) compared to the two other sites dominated by hard coral.

Additionally, the deeper deployment depth, which was chosen due to the lack of coral assemblages at shallower depths where a steep rocky wall borders the shore, likely contributed to reduced NEP due to lower light levels and lower water temperatures found in a couple of meters deeper water. The observations at Sham Wan highlight the likelihood that, as coral abundance and overall diversity decline westward across Hong Kong (Duprey et al., 2016, 2020; McIlroy et al, 2024), the metabolic activity of the benthic community likely decreases. Lower abundance communities, similar to Sham Wan, likely encapsulate the declines in coral community NEP expected with westward movement across Hong Kong as both water quality and coral abundance decline.

However, improved water quality and high coral cover does not uniformly equate to positive rates of productivity (Takeshita et al., 2016; Shamberger et al., 2018; Khrizman et al., 2025) if other local environmental variables act to suppress

NEP. Despite TPC being described as one of Hong Kong's most diverse and abundant coral communities (Chui and Ang, 2017), NEP values there were net respiring during this study. Nighttime respiration processes (Nighttime NEP_{mean} = –1.35 ± 1.90 mmol O_2 m^{-2} hr^{-1}) outweighed the daytime productivity (Daytime NEP_{mean} = 0.46 ± 1.90 mmol O_2 m^{-2} hr^{-1}) occurring at this site. Coral bleaching was also recorded at Tung Ping Chau in July and August, due in large part to the warm temperatures seen during the summer of 2022 (Zhao et al., 2023). Following bleaching events, community NEP may be suppressed and may shift systems to net respiration (Hughes and Grottoli, 2013; Courtney et al., 2018; Khrizman et al., 2025). But community-scale responses to bleaching are variable and context dependent, with several studies reporting little to no change in NEP rates following bleaching events (McMahon et al., 2019; Pisapia et al., 2019; Lantz et al., 2022). Additionally, most corals were recorded as recovered, with minimal mortality by November 2022 (AFCD, 2022), which is in agreement with a recent review study that shows that coral communities with persistently low NEP have increased potential for recovery from disturbance events such as bleaching as a result of an increased baseline reliance on heterotrophic processes (Allgeier, 2024). Bleaching is only one of several local variables likely to act in combination to suppress NEP at this site, including low-light and potentially external nutrient inputs stimulating respiration.

While Tung Ping Chau exhibited consistently net-respiring conditions, Sharp Island was the only site to average net productivity, doing so in both the dry season (NEP_{mean} = 0.12 ± 1.28 mmol O_2 m^{-2} hr^{-1}) and in October in the wet season (NEP_{mean} = 0.15 ± 9.38 mmol O_2 m^{-2} hr^{-1}). However, this site also showed significantly greater metabolic variability than the other two sites, with greater productivity signals during the day but also large respiration signals at night. During the wet season, nighttime oxygen depletion was so extreme that during certain hours, periods of moderate to severe hypoxia (61-92 µmol kg^{-1}) (Pezner et al., 2023), reaching levels as low as 70.98 µmol kg^{-1}, occurred, and persisted for up to several hours at a time (Figure S3b,c). This oxygen depletion at Sharp Island could be a result of upwelling of oxygen-depleted water from offshore, as was seen in the CTD cast conducted at Sharp Island, or from in-situ respiration processes occurring within the community. Regardless, hypoxic conditions measured over the benthos at Sharp Island warrant further investigation as they are a cause for a concern for coral at the site, with prolonged exposure to low oxygen conditions shown to have negative effects on coral physiology and function (Pezner et al., 2023).

4.2 Future directions to sustain Hong Kong coral communities

Hong Kong coral communities live under marginal local environmental conditions and have been subject to a mix of anthropogenic and natural stressors that have contributed to their strong resilience and persistence (Goodkin et al., 2011), while also reducing their structural complexity and spatial coverage (Cybulski et al., 2020). This study demonstrates that these communities have generally reduced organic carbon cycling across the east-west gradient yet still persist as functional communities. These findings suggest that persistence in this system may rely on mechanisms other than high net autotrophic production.

Therefore, Hong Kong corals may offer a glimpse into how coral communities may change in response to marginal environmental conditions that are expected to prevail more widely in the future (Camp et al., 2018). Corals have already begun

shifting their distributions poleward (Price et al., 2019) as the equatorial tropics pass thermal limits for coral survival (but see Huang et al., 2024, where other factors, such as aragonite and calcite saturation states under future ocean acidification, may contribute to inhibit poleward migration). Additionally, as coastal areas become increasingly influenced by the effects of urbanization (Hugo, 2011), studying how sub-tropical, urbanized corals are persisting under already marginal environmental conditions is a critical area of research (Schoepf et al., 2023).

By gathering empirical data on NEP rates at high temporal resolution over coral communities around Hong Kong, this study improves our understanding of which local conditions influence the degree of marginality that corals are subject to within a larger highly urbanized marine ecosystem, such as hydrodynamics (Grimaldi et al., 2023), depth (Page et al., 2019; Cyronak et al., 2020), benthic composition (Page et al., 2017), or nutrient levels (Becker et al., 2021). There is still a need for further characterization of NEP across a wider range of reef environments to gain a better understanding of what specific local factors influence the balance between net respiration and net production of coral communities (Khrizman et al., 2025), as it still not clear how this metabolic balance will shift under future climate change.

While NEP provides critical information on organic carbon cycling, future work may benefit from pairing NEP with NEC (net ecosystem calcification) measurements to determine whether net respiration is associated with reduced calcification, enhanced dissolution, or altered carbonate balance (Shamberger et al., 2011; DeCarlo et al., 2017). Measuring coral community metabolism in terms of both NEP and NEC in this type of environment can provide critical insights into what environmental drivers assist the overall community (not just corals) to persist even with net respiration and possibly low community calcification rates, and how these drivers may change over space and time. This includes all metabolically active organisms contributing to enhanced biodiversity found in coral habitats, such as fishes, algae, and bioeroders like urchins and other bivalves. These have been reported as an overlooked but vital part of the community that can directly influence coral growth rates in Hong Kong (Yeung et al., 2021).

Future studies aiming to measure in-situ community NEP in Hong Kong and similar environments may also consider utilizing an approach with paired flux quantification. Recent studies have begun to utilize paired GF-aquatic eddy covariance deployments (Coogan et al., 2022; Khrizman et al., 2025; Boles et al., 2026) in order to quantify NEP at higher temporal resolution and fill in time gaps where GF assumptions are violated. This approach also allows for a comparison of the flux measurements between the GF and eddy covariance to ensure higher confidence in calculated flux rates.

Paired NEP–NEC measurements could also help future studies evaluate whether sites with low or negative NEP differ in calcification, dissolution, or carbonate balance, and thereby provide a stronger basis for assessing restoration potential. However, the present study does not measure NEC and therefore cannot determine whether these communities are accreting, dissolving, or suitable for restoration on the basis of carbonate balance. Our results instead suggest that even coral communities with moderate to high coral cover in eastern Hong Kong can experience low or negative short-term community-scale NEP. Future restoration assessments in Hong Kong would therefore benefit from integrating NEP, NEC, benthic composition, hydrodynamics, light availability, and longer-term ecological monitoring, particularly at locations where restoration projects

have already been carried out, such as Tolo Harbour (World Wildlife Fund, 2025), Bluff Island (ARCHIREEF, 2025) and Hoi Ha Wan (AFCD, 2019).

5 Conclusions

Even under marginal environmental conditions, community-scale organic carbon cycling varies markedly seasonally and in response to small-scale variations in local conditions. Within the periods suitable for GF calculation, this study demonstrated such variability in NEP signals over coral communities persisting under a suite of local stressors in Hong Kong. NEP rates were negative or only slightly positive for all sites and both seasons, consistent with constrained net organic carbon production at the community scale. Wet season NEP was lower and more variable than the dry season at all three study sites. These suppressed NEP rates indicate that coral communities across Hong Kong have persisted with moderate to high coral cover despite low or negative short-term community-scale NEP, likely reflecting a combination of chronic low-light limitation, external organic matter input stimulating heterotrophic feeding, benthic respiration and seasonal variability.

More studies investigating metabolic patterns of coral communities subject to highly variable and marginal environmental conditions will increase the data available to model and predict future changes in coral ecosystem functioning in response to climate change and local stressors. Furthermore, such data and models can help to identify marine environments that are more suited for management efforts and restoration projects, or conversely unlikely to support functioning coral communities in the future. We advocate for more widespread collection of concurrent high-temporal-resolution, in-situ biophysical and metabolic data over coral communities across the globe to further our knowledge of community-level organic metabolism under marginal conditions likely to dominate coastal habitats in the future.

Data availability

Environmental water quality data around Hong Kong can be obtained from the Environmental Protection Department (EPD; https://cd.epic.epd.gov.hk/EPICRIVER/marine/?lang=en), while weather observations are provided by Hong Kong Observatory (HKO; https://www.hko.gov.hk). Environmental and community composition data collected during this study are archived in Zenodo at https://doi.org/10.5281/zenodo.21696900.

Supplement link

Supplementary Information attached.

Author contributions

T.B.K.: Conceptualization (equal), Data curation (lead), Formal Analysis (lead) Investigation (lead), Methodology (lead), Project Administration (supporting), Validation (lead), Visualization (lead), Writing – Original Draft Preparation (lead), Writing – Review & Editing (lead). **Y-D.P.:** Formal Analysis (supporting), Investigation (supporting), Methodology (supporting), Project Administration (supporting), Writing – Review & Editing (supporting). **J.B-W.:** Investigation (supporting), Project Administration (supporting). **A.S.J.W.:** Conceptualization (equal), Data curation (supporting), Funding Acquisition (lead), Investigation (supporting), Methodology (supporting), Project Administration (lead), Resources (lead), Supervision (lead), Writing – Original Draft Preparation (supporting), Writing – Review & Editing (supporting).

Competing interests

The authors have declared no competing interests.

Disclaimer

Copernicus Publications remains neutral with regard to jurisdictional claims made in the text, published maps, institutional affiliations, or any other geographical representation in this paper. While Copernicus Publications makes every effort to include appropriate place names, the final responsibility lies with the authors. Views expressed in the text are those of the authors and do not necessarily reflect the views of the publisher.

Acknowledgements

Thank you to C. Skinner for assistance with early field seasons and to the skilled boat captains C. W. Wong, I. Kwok, and V. Tong for field work support. Field deployments were performed under permits '(47) in AF MPD 09/3 Pt.24', '(2) in AF MPD 09_3 Pt.25', and '(27) in AF MPD 09_3 Pt.25' from the Hong Kong Agriculture, Fisheries and Conservation Department (AFCD).

Financial support

The work was partially supported by funding from the Hong Kong Branch of the Southern Marine Science and Engineering Laboratory Guangdong Laboratory (Guangzhou) (SMSEGL20SC01) and Research Grants Council (RGC) of Hong Kong (RGC project number AoE/P-601/23-N). TK, YDP, and JBW were supported by the RGC Hong Kong PhD Fellowship Scheme (HKPFS PF19-35625, PF22-74876, and PF21-66378, respectively).

678 **References**

679 Agriculture, Fisheries and Conservation Department (AFCD): Hard coral restoration in Hoi Ha Wan Marine Park (Part 1),
680 https://www.afcd.gov.hk/english/country/cou_vis/cou_vis_mar/cou_vis_mar_mon/files/HCR_e.pdf (last access: 2
681 August 2024), 2019.

682 Agriculture, Fisheries and Conservation Department (AFCD): Hong Kong Reef Check 2022,
683 https://www.afcd.gov.hk/english/conservation/con_mar/con_mar_cor/con_mar_cor_hkrc/files/HKRC_2022_Results_Su
684 mmary_Eng.pdf (last access: 23 February 2025), 2022.

685 Allgeier, J. E.: The ecosystem ecology of coral reefs revisited, Annu. Rev. Ecol. Evol. Syst., 55, 251-370, 2024.

686 Andersson, A. J. and Gledhill, D.: Ocean acidification and coral reefs: effects on breakdown, dissolution, and net ecosystem
687 calcification, Annual Review of Marine Science, 5, 321–348, https://doi.org/10.1146/annurev-marine-121211-172241,
688 2013.

689 ARCHIREEF: Sino Group Harbour of Love, https://archireef.co/sino-group/ (last access: 15 April 2025), 2025.

690 Barnas, D. M., Zeff, M., and Silbiger, N. J.: Submarine groundwater discharge drives both direct and indirect effects on
691 organismal and community metabolism on coral reefs, Proc. R. Soc. B, 292, 2039, 2025.

692 Becker, D. M., Putnam, H. M., Burkepile, D. E., Adam, T. C., Vega Thurber, R., and Silbiger, N. J.: Chronic low-level nutrient
693 enrichment benefits coral thermal performance in a fore reef habitat, Coral Reefs, 40, 1637–1655,
694 https://doi.org/10.1007/s00338-021-02138-2, 2021.

695 Beijbom, O., Edmunds, P. J., Roelfsema, C., et al.: Towards automated annotation of benthic survey images: variability of
696 human experts and operational modes of automation, PLoS ONE, 10, e0130312,
697 https://doi.org/10.1371/journal.pone.0130312, 2015.

698 Bessell-Browne, P., Negri, A. P., Fisher, R., Clode, P. L., and Jones, R.: Impacts of light limitation on corals and crustose
699 coralline algae, Sci. Rep., 7, 11553, 2017.

700 Boles, E., Khrizman, A., Hamilton, J., Mucciarone, D., Koseff, J., Dunbar, R., and Monismith, S.: Measuring metabolic fluxes
701 on shallow, wavy coral reefs, J. Geophys. Res.-Oceans, 131, e2025JC022922, 2026.

702 Brandl, S. J., Rasher, D. B., Côté, I. M., Casey, J. M., Darling, E. S., Lefcheck, J. S., and Duffy, J. E.: Coral reef ecosystem
703 functioning: eight core processes and the role of biodiversity, Front. Ecol. Environ., 17, 445-454, 2019.

704 Browne, N. K., Precht, E., Last, K. S., and Todd, P. A.: Photo-physiological costs associated with acute sediment stress events
705 in three near-shore turbid water corals, Mar. Ecol. Prog. Ser., 502, 129-143, 2014.

706 Cacciapaglia, C. and van Woesik, R.: Reef-coral refugia in a rapidly changing ocean, Glob. Change Biol., 21, 2272-2282,
707 2015.

708 Camp, E. F., Schoepf, V., Mumby, P. J., Hardtke, L. A., Rodolfo-Metalpa, R., Smith, D. J., and Suggett, D. J.: The future of
709 coral reefs subject to rapid climate change: lessons from natural extreme environments, Frontiers in Marine Science, 5, 4,
710 https://doi.org/10.3389/fmars.2018.00004, 2018.

711 Cheung-Wong, R. W., Dytnerski, J. K., Gotama, R., Hemraj, D. A., and Russell, B. D.: Seasonal patterns of macroalgal and
712 sessile invertebrate communities in a monsoonal marine ecosystem, Estuarine, Coastal and Shelf Science, 275, 107962,
713 https://doi.org/10.1016/j.ecss.2022.107962, 2022.

714 Chui, A. P. Y. and Ang Jr., P.: Recruitment failure of scleractinian corals in a subtropical marginal environment: three-year
715 monitoring in a Hong Kong marine park, Mar. Pollut. Bull., 124, 668-677, 2017.

716 Chung, S. S., Au, A., and Qiu, J. W.: Understanding the underwater behaviour of scuba divers in Hong Kong, Environmental
717 Management, 51, 824–837, https://doi.org/10.1007/s00267-013-0023-y, 2013.

718 Chung, T. H., Dellisanti, W., Lai, K. P., Wu, J., Qiu, J. W., and Chan, L. L.: Local conditions modulated the effects of marine
719 heatwaves on coral bleaching in subtropical Hong Kong waters, Coral Reefs, 43, 1235–1247,
720 https://doi.org/10.1007/s00338-024-02533-5, 2024.

721 Coles, S. L. and Jokiel, P. L.: Effects of salinity on coral reefs, in: Pollution in Tropical Aquatic Systems, CRC Press, 147-
722 166, 2018.

723 Coogan, J., Rheuban, J. E., and Long, M. H.: Evaluating benthic flux measurements from a gradient flux system, Limnology
724 and Oceanography: Methods, https://doi.org/10.1002/lom3.10482, 2022.

725 Courtney, T. A., De Carlo, E. H., Page, H. N., Bahr, K. D., Barro, A., Howins, N., et al.: Recovery of reef-scale calcification
726 following a bleaching event in Kāne'ohe Bay, Hawai'i, Limnol. Oceanogr. Lett., 3, 1-9, 2018.

727 Cybulski, J. D., Husa, S. M., Duprey, N. N., et al.: Coral reef diversity losses in China's Greater Bay Area were driven by
728 regional stressors, Science Advances, 6, eabb1046, https://doi.org/10.1126/sciadv.abb1046, 2020.

729 Cyronak, T., Andersson, A. J., Langdon, C., et al.: Taking the metabolic pulse of the world's coral reefs, PLoS ONE, 13,
730 e0190872, https://doi.org/10.1371/journal.pone.0190872, 2018.

731 Cyronak, T., Takeshita, Y., Courtney, T. A., et al.: Diel temperature and pH variability scale with depth across diverse coral
732 reef habitats, Limnology and Oceanography Letters, 5, 193–203, https://doi.org/10.1002/lol2.10129, 2020.

733 D'Angelo, C. and Wiedenmann, J.: Impacts of nutrient enrichment on coral reefs: new perspectives and implications for coastal
734 management and reef survival, Curr. Opin. Environ. Sustain., 7, 82-93, 2014.

DeCarlo, T. M., Cohen, A. L., Wong, G. T., et al.: Community production modulates coral reef pH and the sensitivity of ecosystem calcification to ocean acidification, Journal of Geophysical Research: Oceans, 122, 745–761, https://doi.org/10.1002/2016JC012326, 2017.

Dellisanti, W., Tsang, R. H. L., Ang, P., Wu, J., Wells, M. L., and Chan, L. L.: A diver-portable respirometry system for in-situ short-term measurements of coral metabolic health and rates of calcification, Frontiers in Marine Science, 7, 571451, https://doi.org/10.3389/fmars.2020.571451, 2020.

Dennison, W. C. and Barnes, D. J.: Effect of water motion on coral photosynthesis and calcification, J. Exp. Mar. Biol. Ecol., 115, 67-77, 1988.

Doney, S. C., Fabry, V. J., Feely, R. A., and Kleypas, J. A.: Ocean acidification: the other CO2 problem, Annual Review of Marine Science, 1, 169–192, https://doi.org/10.1146/annurev.marine.010908.163834, 2009.

Dumont, C. P., Lau, D. C. C., Astudillo, J. C., Fong, K. F., Chak, S. T. C., and Qiu, J. W.: Coral bioerosion by the sea urchin Diadema setosum in Hong Kong: susceptibility of different coral species, Journal of Experimental Marine Biology and Ecology, 441, 71–79, https://doi.org/10.1016/j.jembe.2013.01.018, 2013.

Duprey, N. N., McIlroy, S. E., Ng, T. P. T., et al.: Facing a wicked problem with optimism: issues and priorities for coral conservation in Hong Kong, Biodiversity and Conservation, 26, 2521–2545, https://doi.org/10.1007/s10531-017-1383-z, 2017.

Duprey, N. N., Wang, T. X., Kim, T., et al.: Megacity development and the demise of coastal coral communities: evidence from coral skeleton δ15N records in the Pearl River estuary, Global Change Biology, 26, 1338–1353, https://doi.org/10.1111/gcb.14923, 2020.

Duprey, N. N., Yasuhara, M., and Baker, D. M.: Reefs of tomorrow: eutrophication reduces coral biodiversity in an urbanized seascape, Global Change Biology, 22, 3550–3565, https://doi.org/10.1111/gcb.13302, 2016.

Edmunds, P. J., Comeau, S., Lantz, C., et al.: Integrating the effects of ocean acidification across functional scales on tropical coral reefs, BioScience, 66, 350–362, https://doi.org/10.1093/biosci/biw023, 2016.

Falter, J. L., Atkinson, M. J., Schar, D. W., Lowe, R. J., and Monismith, S. G.: Short-term coherency between gross primary production and community respiration in an algal-dominated reef flat, Coral Reefs, 30, 53-58, 2011.

Falter, J. L., Lowe, R. J., Atkinson, M. J., and Cuet, P.: Seasonal coupling and de-coupling of net calcification rates from coral reef metabolism and carbonate chemistry at Ningaloo Reef, Western Australia, Journal of Geophysical Research: Oceans, 117, C05003, https://doi.org/10.1029/2011JC007268, 2012.

Falter, J. L., Lowe, R. J., Atkinson, M. J., Monismith, S. G., and Schar, D. W.: Continuous measurements of net production over a shallow reef community using a modified Eulerian approach, J. Geophys. Res.-Oceans, 113, C07035, 2008.

765 Ferrier-Pages, C., Gattuso, J. P., and Jaubert, J.: Effect of small variations in salinity on the rates of photosynthesis and
766 respiration of the zooxanthellate coral Stylophora pistillata, Mar. Ecol. Prog. Ser., 181, 309-314, 1999.

767 Gattuso, J. P., Pichon, M., Jaubert, J., Marchioretti, M., and Frankignoulle, M.: Primary production, calcification and air-sea
768 CO2 fluxes in coral reefs: organism, ecosystem and global scales, Bull. Inst. Oceanogr. Monaco, 14, 1996.

769 Goatley, C. H. and Bellwood, D. R.: The roles of dimensionality, canopies and complexity in ecosystem monitoring, PLoS
770 ONE, 6, e27307, 2011.

771 Goodkin, N. F., Switzer, A. D., McCorry, D., et al.: Coral communities of Hong Kong: long-lived corals in a marginal reef
772 environment, Marine Ecology Progress Series, 426, 185–196, https://doi.org/10.3354/meps09019, 2011.

773 Grimaldi, C. M., Lowe, R. J., Benthuysen, J. A., Cuttler, M. V. W., Green, R. H., and Gilmour, J. P.: Hydrodynamic and
774 atmospheric drivers create distinct thermal environments within a coral reef atoll, Coral Reefs, 42, 693–706,
775 https://doi.org/10.1007/s00338-023-02371-x, 2023.

776 Gross, T. F. and Nowell, A. R.: Mean flow and turbulence scaling in a tidal boundary layer, Continental Shelf Research, 2,
777 109–126, https://doi.org/10.1016/0278-4343(83)90011-0, 1983.

778 Haapkylä, J., Unsworth, R. K., Flavell, M., Bourne, D. G., Schaffelke, B., and Willis, B. L.: Seasonal rainfall and runoff
779 promote coral disease on an inshore reef, PLoS ONE, 6, e16893, 2011.

780 Heery, E. C., Hoeksema, B. W., Browne, N. K., et al.: Urban coral reefs: degradation and resilience of hard coral assemblages
781 in coastal cities of East and Southeast Asia, Marine Pollution Bulletin, 135, 654–681,
782 https://doi.org/10.1016/j.marpolbul.2018.07.041, 2018.

783 Hochberg, E. J., Pisapia, C., Carpenter, R. C., and Hall, S.: Light-use efficiency for coral reef communities and benthic
784 functional types, Limnol. Oceanogr., 69, 712-722, 2024.

785 Hong Kong Environment Protection Department (EPD): https://cd.epic.epd.gov.hk/EPICRIVER/marine/?lang=en (last access
786 15 December 2023), 2023.

787 Hong Kong Observatory: Hourly meteorological data for Hong Kong, including rainfall, temperature, wind, and solar radiation
788 (2013–2022), https://www.hko.gov.hk (last access: 9 September 2024), 2025.

789 Hong Kong Observatory: Solar energy resources in Hong Kong from a climatological point of view,
790 https://www.hko.gov.hk/en/education/weather/sunshine-and-uv/00443-solar-energy-resources-in-hong-kong-from-a-
791 climatological-point-of-view.html (last access: 21 December 2024), 2022.

792 Huang, Y. Y., Chen, T. R., Lai, K. P., et al.: Poleward migration of tropical corals inhibited by future trends of seawater
793 temperature and calcium carbonate (CaCO3) saturation, Science of the Total Environment, 929, 172562,
794 https://doi.org/10.1016/j.scitotenv.2024.172562, 2024.

Hughes, A. D. and Grottoli, A. G.: Heterotrophic compensation: a possible mechanism for resilience of coral reefs to global warming or a sign of prolonged stress?, PLoS ONE, 8, e81172, 2013.

Hughes, T. P., Kerry, J. T., Álvarez-Noriega, M., et al.: Global warming and recurrent mass bleaching of corals, Nature, 543, 373–377, https://doi.org/10.1038/nature21707, 2017.

Hugo, G.: Future demographic change and its interactions with migration and climate change, Global Environmental Change, 21, S21–S33, https://doi.org/10.1016/j.gloenvcha.2011.09.008, 2011.

Kayanne, H., Hata, H., Kudo, S., Yamano, H., Watanabe, A., Ikeda, Y., et al.: Seasonal and bleaching-induced changes in coral reef metabolism and CO2 flux, Global Biogeochem. Cy., 19, GB3015, 2005.

Kekuewa, S. A. H., Courtney, T. A., Cyronak, T., et al.: Temporal and spatial variabilities of chemical and physical parameters on the Heron Island coral reef platform, Aquatic Geochemistry, https://doi.org/10.1007/s10498-021-09400-7, 2021.

Kelly, L. W., Williams, G. J., Barott, K. L., Carlson, C. A., Dinsdale, E. A., Edwards, R. A., et al.: Local genomic adaptation of coral reef-associated microbiomes to gradients of natural variability and anthropogenic stressors, Proc. Natl. Acad. Sci. USA, 111, 10227-10232, 2014.

Khrizman, A., Lindhart, M., Mucciarone, D. A., Takeshita, Y., Monismith, S. G., Boles, E. L., and Dunbar, R. B.: Reef community productivity and calcification–spatial and temporal variability in recovering coral reefs, Journal of Geophysical Research: Oceans, 130, e2024JC021592, https://doi.org/10.1029/2024JC021592, 2025.

Lantz, C. A., Leggat, W., Bergman, J. L., Fordyce, A., Page, C., Mesaglio, T., and Ainsworth, T. D.: Will daytime community calcification reflect reef accretion on future, degraded coral reefs?, Biogeosciences, 19, 891-906, 2022.

Law, M. T. and Huang, D.: Light limitation and coral mortality in urbanised reef communities due to sea-level rise, Climate Change Ecology, 5, 100073, https://doi.org/10.1016/j.ecochg.2023.100073, 2023.

Long, M. H., Berg, P., de Beer, D., and Zieman, J. C.: In situ coral reef oxygen metabolism: an eddy correlation study, PLoS ONE, 8, e58581, 2013.

Lowe, A. T., Bos, J., and Ruesink, J.: Ecosystem metabolism drives pH variability and modulates long-term ocean acidification in the Northeast Pacific coastal ocean, Scientific Reports, 9, 963, https://doi.org/10.1038/s41598-018-37764-4, 2019.

Manzello, D. and Lirman, D.: The photosynthetic resilience of Porites furcata to salinity disturbance, Coral Reefs, 22, 537-540, 2003.

McGillis, W. R., Langdon, C., Loose, B., Yates, K. K., and Corredor, J.: Productivity of a coral reef using boundary layer and enclosure methods, Geophysical Research Letters, 38, L03611, https://doi.org/10.1029/2010GL046179, 2011.

McIlroy, S. E., Guibert, I., Archana, A., et al.: Life goes on: spatial heterogeneity promotes biodiversity in an urbanized coastal marine ecosystem, Global Change Biology, 30, e17248, https://doi.org/10.1111/gcb.17248, 2024.

McIlroy, S. E., Thompson, P. D., Yuan, F. L., Bonebrake, T. C., and Baker, D. M.: Subtropical thermal variation supports persistence of corals but limits productivity of coral reefs, Proceedings of the Royal Society B, 286, 20190882, https://doi.org/10.1098/rspb.2019.0882, 2019.

McMahon, A., Santos, I. R., Schulz, K. G., Scott, A., Silverman, J., Davis, K. L., and Maher, D. T.: Coral reef calcification and production after the 2016 bleaching event at Lizard Island, Great Barrier Reef, J. Geophys. Res.-Oceans, 124, 4003-4016, 2019.

Meléndez, M., Salisbury, J., Gledhill, D., Langdon, C., Morell, J. M., Manzello, D., and Sutton, A.: Net ecosystem dissolution and respiration dominate metabolic rates at two western Atlantic reef sites, Limnol. Oceanogr., 67, 527-539, https://doi.org/10.1002/lno.12009, 2022.

Moberg, F. and Folke, C.: Ecological goods and services of coral reef ecosystems, Ecological Economics, 29, 215–233, https://doi.org/10.1016/S0921-8009(99)00009-9, 1999.

Moberg, F., Nyström, M., Kautsky, N., Tedengren, M., and Jarayabhand, P.: Effects of reduced salinity on the rates of photosynthesis and respiration in the hermatypic corals Porites lutea and Pocillopora damicornis, Mar. Ecol. Prog. Ser., 157, 53-59, 1997.

Morgan, K. M., Moynihan, M. A., Sanwlani, N., and Switzer, A. D.: Light limitation and depth-variable sedimentation drives vertical reef compression on turbid coral reefs, Front. Mar. Sci., 7, 571256, https://doi.org/10.3389/fmars.2020.571256, 2020.

Morgan, K. M., Perry, C. T., Johnson, J. A., and Smithers, S. G.: Nearshore turbid-zone corals exhibit high bleaching tolerance on the Great Barrier Reef following the 2016 ocean warming event, Frontiers in Marine Science, 4, 224, https://doi.org/10.3389/fmars.2017.00224, 2017.

Morton, B.: Pollution of the coastal waters of Hong Kong, Marine Pollution Bulletin, 20, 310–318, https://doi.org/10.1016/0025-326X(89)90153-7, 1989.

NASA Langley Research Center (LaRC), POWER Project: Surface meteorology and solar energy data for the Caribbean region (NASA SSE v4.0), https://power.larc.nasa.gov (last access: 1 June 2024), 2025.

Nelson, H. R. and Altieri, A. H.: Oxygen: the universal currency on coral reefs, Coral Reefs, 38, 177-198, 2019.

Nilsson, G. E., Östlund-Nilsson, S., and Munday, P. L.: Effects of elevated temperature on coral reef fishes: loss of hypoxia tolerance and inability to acclimate, Comp. Biochem. Physiol. A, 156, 389-393, 2010.

Odum, H. T. and Odum, E. P.: Trophic structure and productivity of a windward coral reef community on Eniwetok Atoll, Ecol. Monogr., 25, 291-320, 1955.

Page, H. N., Courtney, T. A., Collins, A., DeCarlo, E. H., and Andersson, A. J.: Net community metabolism and seawater carbonate chemistry scale non-intuitively with coral cover, Frontiers in Marine Science, 4, 161, https://doi.org/10.3389/fmars.2017.00161, 2017.

Page, H. N., Courtney, T. A., DeCarlo, E. H., Howins, N. M., Koester, I., and Andersson, A. J.: Spatiotemporal variability in seawater carbon chemistry for a coral reef flat in Kāneʻohe Bay, Hawaiʻi, Limnology and Oceanography, 64, 913–934, https://doi.org/10.1002/lno.11084, 2019.

Parry, A. J., Klein, S. G., and Duarte, C. M.: Thermal extremes likely trigger metabolic imbalance in coral holobionts, Sci. Rep., 15, 33181, 2025.

Pezner, A. K., Courtney, T. A., Barkley, H. C., Chou, W. C., Chu, H. C., Clements, S. M., ... and Andersson, A. J.: Increasing hypoxia on global coral reefs under ocean warming, Nature Climate Change, 13, 403–409, https://doi.org/10.1038/s41558-023-01619-2, 2023.

Pisapia, C., Hochberg, E. J., and Carpenter, R.: Multi-decadal change in reef-scale production and calcification associated with recent disturbances on a Lizard Island reef flat, Front. Mar. Sci., 6, 575, 2019.

Platz, M. C., Arias, M. E., and Byrne, R. H.: Reef metabolism monitoring methods and potential applications for coral restoration, Environmental Management, 69, 612–625, https://doi.org/10.1007/s00267-022-01597-9, 2022.

Platz, M. C., Takeshita, Y., Bartels, E., and Arias, M. E.: Evaluating the potential for autonomous measurements of net community production and calcification as a tool for monitoring coral restoration, Ecological Engineering, 158, 106042, https://doi.org/10.1016/j.ecoleng.2020.106042, 2020.

Price, N. N., Muko, S., Legendre, L., et al.: Global biogeography of coral recruitment: tropical decline and subtropical increase, Marine Ecology Progress Series, 621, 1–17, https://doi.org/10.3354/meps12980, 2019.

Qiu, J. W., Lau, D. C., Cheang, C. C., and Chow, W. K.: Community-level destruction of hard corals by the sea urchin Diadema setosum, Mar. Pollut. Bull., 85, 783-788, 2014.

Riegl, B. and Branch, G. M.: Effects of sediment on the energy budgets of four scleractinian (Bourne 1900) and five alcyonacean (Lamouroux 1816) corals, J. Exp. Mar. Biol. Ecol., 186, 259-275, 1995.

Rosedy, A., Ives, I., Waheed, Z., Hussein, M. A. S., Sosdian, S., Johnson, K., and Santodomingo, N.: Turbid reefs experience lower coral bleaching effects in NE Borneo (Sabah, Malaysia), Reg. Stud. Mar. Sci., 68, 103268, 2023.

Roth, M. S.: The engine of the reef: photobiology of the coral-algal symbiosis, Front. Microbiol., 5, 422, 2014.

Sawall, Y., Teichberg, M. C., Seemann, J., Litaay, M., Jompa, J., and Richter, C.: Nutritional status and metabolism of the coral Stylophora subseriata along a eutrophication gradient in Spermonde Archipelago (Indonesia), Coral Reefs, 30, 841-853, 2011.

Schoepf, V., Baumann, J. H., Barshis, D. J., et al.: Corals at the edge of environmental limits: a new conceptual framework to re-define marginal and extreme coral communities, Science of the Total Environment, 884, 163688, https://doi.org/10.1016/j.scitotenv.2023.163688, 2023.

Shamberger, K. E. F., Feely, R. A., Sabine, C. L., Atkinson, M. J., DeCarlo, E. H., Mackenzie, F. T., et al.: Calcification and organic production on a Hawaiian coral reef, Mar. Chem., 127, 64-75, 2011.

Shamberger, K. E., Lentz, S. J., and Cohen, A. L.: Low and variable ecosystem calcification in a coral reef lagoon under natural acidification, Limnol. Oceanogr., 63, 714-730, 2018.

Silbiger, N. J., Nelson, C. E., Remple, K., Sevilla, J. K., Quinlan, Z. A., Putnam, H. M., et al.: Nutrient pollution disrupts key ecosystem functions on coral reefs, Proc. R. Soc. B, 285, 1880, 2018.

SolarGIS s.r.o.: Solar radiation data for the Red Sea (1 January 2013–31 December 2022), https://solargis.com (last access: 1 June 2024), 2025.

Solcast Pty Ltd.: Solar irradiance data for the Great Barrier Reef (1 January 2013–31 December 2022), https://solcast.com (last access: 1 June 2024), 2025.

Stoltenberg, L., Schulz, K. G., Cyronak, T., and Eyre, B. D.: Seasonal variability of calcium carbonate precipitation and dissolution in shallow coral reef sediments, Limnology and Oceanography, 65, 876–891, https://doi.org/10.1002/lno.11357, 2020.

Suarez, J. D. U., Wong, J. C., Dumont, C. P., and Qiu, J. W.: High density and secondary production but variable recruitment of a sea urchin in subtidal barren areas of Hong Kong, Reg. Stud. Mar. Sci., 48, 102027, 2021.

Sully, S. and van Woesik, R.: Turbid reefs moderate coral bleaching under climate-related temperature stress, Global Change Biology, 26, 1367–1373, https://doi.org/10.1111/gcb.14948, 2020.

Takeshita, Y., Cyronak, T., Martz, T. R., Kindeberg, T., and Andersson, A. J.: Coral reef carbonate chemistry variability at different functional scales, Frontiers in Marine Science, 5, 175, https://doi.org/10.3389/fmars.2018.00175, 2018.

Takeshita, Y., McGillis, W., Briggs, E., et al.: Coral reef metabolism using a boundary layer approach, Journal of Geophysical Research: Oceans, 121, 5655–5671, https://doi.org/10.1002/2016JC011886, 2016.

Tran, L. L. and Johansen, J. L.: Seasonal variability in resilience of a coral reef fish to marine heatwaves and hypoxia, Glob. Change Biol., 29, 2522-2535, 2023.

Travaglione, N., Evans, R., Moustaka, M., et al.: Scleractinian corals rely on heterotrophy in highly turbid environments, Coral Reefs, 42, 997–1010, https://doi.org/10.1007/s00338-023-02407-2, 2023.

Turk, D., Yates, K. K., Vega-Rodriguez, M., et al.: Community metabolism in shallow coral reef and seagrass ecosystems, lower Florida Keys, Marine Ecology Progress Series, 538, 35–52, https://doi.org/10.3354/meps11385, 2015.

Tuttle, L. J. and Donahue, M. J.: Effects of sediment exposure on corals: a systematic review of experimental studies, Environmental Evidence, 11, 4, https://doi.org/10.1186/s13750-022-00256-0, 2022.

Valino, D. A., Patel, S., and Morgan, K.: Habitat capacity is decoupled from coral cover on turbid reef systems, Ecol. Indic., 187, 114947, 2026.

van Hoytema, N., Bednarz, V. N., Cardini, U., Naumann, M. S., Al-Horani, F. A., and Wild, C.: The influence of seasonality on benthic primary production in a Red Sea coral reef, Mar. Biol., 163, 52, 2016.

Wang, W., Cai, S., Huang, J., Ding, R., and Chen, L.: Variation in the quanta-to-energy ratio of photosynthetically active radiation under the cloudless atmosphere, Atmosphere, 15, 1166, https://doi.org/10.3390/atmos15101166, 2024.

Webb, A. E., de Bakker, D. M., Soetaert, K., da Costa, T., van Heuven, S. M. A. C., van Duyl, F. C., Reichart, G.-J., and de Nooijer, L. J.: Quantifying functional consequences of habitat degradation on a Caribbean coral reef, Biogeosciences, 18, 6501-6516, https://doi.org/10.5194/bg-18-6501-2021, 2021.

World Wildlife Fund: Reviving our corals: reviving corals, reviving our oceans, https://revivingourcorals.wwf.org.hk/ (last access: 17 April 2025), 2025.

Xie, J. Y., Yeung, Y. H., Kwok, C. K., et al.: Localized bleaching and quick recovery in Hong Kong's coral communities, Marine Pollution Bulletin, 153, 110950, https://doi.org/10.1016/j.marpolbul.2020.110950, 2020.

Yeung, Y. H., Xie, J. Y., Kwok, C. K., Kei, K., Ang Jr., P., Chan, L. L., et al.: Hong Kong's subtropical scleractinian coral communities: baseline, environmental drivers and management implications, Mar. Pollut. Bull., 167, 112289, 2021.

Yeung, Y. H., Xie, J. Y., Zhao, Y., et al.: Rapid external erosion of coral substrate in subtropical Hong Kong waters, Marine Pollution Bulletin, 169, 112495, https://doi.org/10.1016/j.marpolbul.2021.112495, 2021.

Yiu, S. K. F., Leung, T. K. T., Lee, G. Y., and Yan, M.: Spatial variation and habitat preference of reef fish and gastropod assemblages from two coastal habitats in subtropical reef, Port Shelter, Hong Kong, Mar. Environ. Res., 107533, 2025.

Zhao, Y., Chen, M., Chung, T. H., Chan, L. L., and Qiu, J. W.: The 2022 summer marine heatwaves and coral bleaching in China's Greater Bay Area, Marine Environmental Research, 189, 106044, https://doi.org/10.1016/j.marenvres.2023.106044, 2023.

938 Zhou, W., Yin, K., Harrison, P. J., and Lee, J. H. W.: The influence of late summer typhoons and high river discharge on water
939 quality in Hong Kong waters, Estuarine, Coastal and Shelf Science, 111, 35–47,
940 https://doi.org/10.1016/j.ecss.2012.06.004, 2012.

941 Zweifler, A., O'Leary, M., Morgan, K., and Browne, N. K.: Turbid coral reefs: past, present and future-a review, Diversity,
942 13, 251, https://doi.org/10.3390/d13060251, 2021.